00387

# UNIVERSIDAD NACIONAL AUTONOMA DE MEXICO

POSGRADO EN CIENCIAS BIOLOGICAS

FACULTAD DE CIENCIAS

## DISECCION MOLECULAR *IN SITU* DEL NUCLEOLO ANCESTRAL.

**T E S I S**

QUE PARA OBTENER EL GRADO ACADEMICO DE:

**DOCTOR EN CIENCIAS**

P R E S E N T A

GABRIEL LOPEZ VELAZQUEZ

DIRECTOR DE TESIS: DR. LUIS FELIPE JIMENEZ GARCIA


MEXICO, D. F. 2004

VNIVERSIDAD NACIONAL
AVPNOMA DE
MEXICO

**POSGRADO EN CIENCIAS BIOLÓGICAS**
**COORDINACIÓN**

Ing. Leopoldo Silva Gutiérrez
Director General de Administración Escolar, UNAM
Presente

Por medio de la presente me permito informar a usted que en la reunión ordinaria del Comité Académico del Posgrado en Ciencias Biológicas, celebrada el dia 7 de junio del 2004, se acordó poner a su consideración el siguiente jurado para el examen de grado del Doctorado en Ciencias del alumno(a) **Gabriel López Velázquez**, con número de cuenta 85383320 y número de expediente 3971056, con la tesis titulada: **"Disección molecular In Situ del nucleolo ancestral"**, bajo la dirección del (la) **Dr. Luis Felipe Jiménez Garcia.**

| | |
|---|---|
| Presidente: | Dr. Antonio Eusebio Lazcano-Araujo Reyes |
| Vocal: | Dr. Horacio Reyes Vivas |
| Vocal: | Dra. Maria Imelda López Villaseñor |
| Vocal: | Dra. Rocio George Téllez |
| Secretario: | Dr. Luis Felipe Jiménez Garcia |
| Suplente: | Dra. Lourdes Segura Valdez |
| Suplente: | René de Jesüs Cárdenas Vàzquez |

Sin otro particular, quedo de usted.

Atentamente
"POR MI RAZA HABLARA EL ESPIRITU"
Cd. Universitaria, D.F., a 23 de junio del 2004

Dr. Juan José Morrone Lupi
Coordinador del Programa

c.c.p. Expediente del interesado

Este trabajo fue realizado en el laboratorio de Microscopía Electrónica de la Facultad de Ciencias de la UNAM, en el laboratorio de Bioquímica Genética del Instituto Nacional de Pediatría y en el laboratorio del Dr. Ramachandra Reddy del Baylor College of Medicine, Houston, Texas, bajo la dirección y asesoría del Dr. Luis Felipe Jiménez García. Se contó con el apoyo de CONACyT J37071-B y PAEP-UNAM 101314. Durante el desarrollo de este trabajo conté con una beca de la DGEP-UNAM para estudios de doctorado, por lo que expreso mi agradecimiento a esta institución.

Agradecimientos:

A Silvia, por su apoyo y por todo el tiempo invertido.
A los miembros del comité tutorial y del jurado por las observaciones a mi trabajo.
A las Dras. Alessandra Carnevale y Sara Frias por su apoyo.
Al Instituto Nacional de Pediatría y sus autoridades por permitirme realizar mis estudios de doctorado.
Al Dr. Horacio Reyes por su amistad y por los conocimientos que me aportó.
Al Dr. Luis Felipe Jiménez por su apoyo y dirección.
Al Dr. Antonio Lazcano por sus excelentes comentarios y apoyo en todo momento.
A todo el personal del laboratorio de Bioquímica Genética: Sara, Dora, Nacho, Gloria y Carmen.
Al laboratorio de Citogenética, especialmente a Bertha Molina por todo su apoyo.
A la Dra. Rosario Ortiz por su apoyo y amistad.
A mis sobrinos: Kayani, Fernanda, Monserrat y José Mar. Ojalá logren todo lo que se propongan.
A mi primo Miguel Ángel, por sus consejos y amistad.
A mis padres.

# Para Bruno

*Ustedes me dicen, entonces, que tengo que perecer*
*como también las flores que cultivé perecerán.*
*¿De mi nombre nada quedará,*
*nadie mi fama recordará?*
*Pero los jardines que planté, son jóvenes y crecerán...*
*Las canciones que canté, ¡cantándose seguirán!*
Huexotzincatzin, 1484

INDICE



**Resumen**

El nucléolo es el sitio donde se lleva a cabo la síntesis y maduración del pre-rRNA en células eucariontes. La mayor parte de la información sobre la organización funcional del nucléolo es a partir de células de mamíferos y plantas, sin embargo no se sabe casi nada acerca de esto en protistas. *Giardia lamblia* es un protista parásito que comparte varias características con procariontes. Esto ha propiciado considerar a *G. lamblia* como un eucarionte de divergencia temprana. Respecto a esto, también hay reportes con relación a la falta de mitocondrias, peroxisomas y nucléolo en este organismo. No obstante, la condición evolutiva de *G. lamblia* está en debate ya que se sabe que en vez de motocondrias posee mitosomas y que hay genes mitocondriales transferidos a núcleo celular. En este sentido, el hecho de presentar fibrilarina, U14 snoRNA, y genes de rDNA organizados en tandem, destaca la importancia de la organización morfológica de estas moléculas el núcleo celular de *G. lamblia*. El objetivo de este trabajo fue analizar la distribución *in situ* de las moléculas involucradas en el procesamiento del pre-rRNA en los núcleos de *G. lamblia*. De manera adicional, se analizaron dos moléculas no relacionadas directamente con el procesamiento del pre-rRNA (gen del U6 snRNA y la enzima triosafosfato isomerasa), pero que se usaron como complemento para entender las características evolutivas de *G. lamblia*. Por otra parte, se estudio y caracterizó el nucléolo de *Trypanosoma cruzi*, tomando en cuenta las similitudes de su nucléolo con el de los eucariontes de divergencia tardía, y su cercanía filogenética con *G. lamblia*. Los resultados mostraron que los núcleos de *G. lamblia* presentan una estructura morfológicamente bien definida, la cual excluye al DNA pero contiene fibrilarina, proteínas nucleolares, y rRNA. Esta estructura representa a un nucléolo con componente granular y fibrilar. La reconstrucción 3D reveló la posición del nucléolo con respecto al núcleo entero. Se clonó un fragmento conservado del gen del U6 snRNA en *G. lamblia*. La triosafosfato isomerasa de este organismo también fue caracterizada. En el caso de *T. cruzi*, el nucléolo se caracterizó ultraestructuralmente y la subcompartamentalización de las moléculas relacionadas con la maduración del rRNA se reporta por primera vez. La reconstrucción 3D mostró un nucléolo por cada núcleo de los epimastigotes de *T. cruzi*, los cuales presentaron una intrincada red compuesta por un componente fibrilar y otro granular.

**Abstract**

Nucleolus is the site where the synthesis and maturation of the pre-rRNA takes place in eukaryotic cells. The bulk of information about functional organization of the nucleolus comes from mammalian and plant cells, but almost nothing is known in protists. *Giardia lamblia* is a parasitic protist that shares several features with prokaryotes. This has propitiated to consider *G. lamblia* as an early diverging eukaryote. It has proposed too that *G. lamblia* lacks mitochondria, peroxisomes and nucleolus. Nonetheless, the presence of mitosomes instead of mitochondria and mitochondrial genes transferred to the nucleus, changed the point of view over the evolutionary status of *G. lamblia*. The presence of fibrillarin, U14 snoRNA like, and tandem rDNA genes, underlines the importance of the morphologic organization of these molecules in the *G. lamblia* nucleus. The aim of this work was to analyze the *in situ* distribution of molecules involved in the rRNA processing in the nuclei of *G. lamblia* and to identify the structures related with them. Additionally, we analyzed two other molecules not related with the rRNA processing (U6 snRNA gene and triosephosphate isomerase) but used them as a complement to understand the evolutionary features of *G. lamblia*. On the other hand, the nucleolus of *Trypanosoma cruzi* was studied and characterized taking into account its similarities with the nucleoli of the most evolutionary derived organisms, and its phylogenetic closeness to *G. lamblia*. The results showed that the nuclei of *G. lamblia* present a structure morphologically defined which excludes DNA and contains fibrillarin, nucleolar proteins, and rRNA. This structure represents a nucleolus showing granular and fibrillar components . 3D reconstructions showed the position of the nucleolus of *G. lamblia* relative to the entire nucleus. A conserved fragment from U6 snRNA gene was cloned from *G. lamblia*. The triosephosphate isomerase was also was characterized. For *T. cruzi*, the nucleolus was ultrastructurally characterized. Molecular and morphological subcompartmentalization related with rRNA metabolism were described. 3D reconstruction showed a single nucleolus per nucleus of *T. cruzi* epimastigotes with an intricate net composed by fibrillar and granular components.

**Abreviaturas**

**ATP**. Trifosfato de adenosina.

**ddATP, ddTTP, ddCTP, ddGTP**. Didesoxiadenosina, didesoxitimidina, didesoxicitidina, y didesoxiguanosina, respectivamente.

**DHAP**. Dihidroxiacetona fosfato.

**DNA**. Ácido desoxiribonucleico.

**ETS**. Espaciador transcrito externo.

**FIGE**. Electroforesis de campo invertido.

**GAP**. Gliceraldehído 3 fosfato.

**gDNA**. DNA genómico

**GITIM**. Triosafosfato isomera de *Giardia lamblia*.

**ITS**. Espaciador transcrito interno.

**TIM**. Triosafosfato isomerasa

**LSRNA**. Subunidad grande de RNA ribosomal

**Mb**. Mega bases.

**nt**. Nucleótidos.

**NTS**. Espaciador no transcrito.

**pb**. Pares de bases.

**PCR**. Reacción en cadena de la polimerasa.

**pol I**. Polimerasa I.

**pre-rRNA**. rRNA precursor.

**rDNA**. Genes ribosomales.

**RNA**. Ácido ribonucleico.

**rRNA**. RNA ribosomal.

**snRNA**. RNA pequeño nuclear.

**snoRNA**. RNA pequeño nucleolar

**SSRNA**. Subunidad pequeña de RNA ribosomal.

**RTPCR**. Reverso transcripción seguida de PCR.

**U1, U2, U4, U5, U6**. RNAs pequeños nucleares ricos en uracilo.

**U3, U14**. RNAs pequeños nucleolares ricos en uracilo.

## I. Introducción

### I.1. Genes ribosomales versus complejidad del genoma

Todos los organismos vivos sin excepción requieren de la síntesis de RNA ribosomal (rRNA) para la formación de los ribosomas, que a su vez serán el substrato morfológico para la síntesis proteica.

El genoma de las mitocondrias de humano contiene solo una copia de los genes 12S y 16S ribosomales. Al parecer esto es suficiente para traducir las trece proteínas codificadas por los genes de este organelo. Los micoplasmas, reconocidos como los procariontes más pequeños ( hasta el descubrimiento de *Nanoarchaeum equitans*), contienen dos juegos de genes ribosomales. El genoma de *Escherichia coli* es de 4 a 5 veces más grande que el de *Mycoplasma capricolum* y solo contiene siete juegos de genes ribosomales. En levaduras el número de genes ribosomales es de aproximadamente 140, en humano 300 copias y en el maíz es de entre 3000 a 9000 copias. Analizando estos datos y los presentados en la tabla 1, se puede sugerir una correlación entre el tamaño del genoma y el número de genes ribosomales (con algunas excepciones como en el maíz y el ciliado *Tetrahymena*).

Se han propuesto dos posibles razones para explicar esta correlación. Una es que simplemente un genoma grande requiere de grandes cantidades de RNA, y la otra es que el número mayor de genes es por simple consecuencia del aumento en el tamaño del genoma y, por consiguiente, de eventos sucesivos de duplicación de genes (en Graur y Li, 2000).

### I.2. Formación del nucléolo

La síntesis y maduración del rRNA requieren de una compleja red de interacciones entre proteínas - proteínas y proteínas - ácidos nucleicos. El sitio en el que se llevan a cabo estos procesos en las células eucariontes es el nucléolo. A pesar de que existen evidencias múltiples de la presencia de dominios funcionales en el nucléolo, se sabe muy poco con relación a las condiciones mínimas necesarias para mantener ensamblados a los factores moleculares que intervienen en los procesos nucleolares. Se ha sugerido que la formación del nucléolo es dirigida por el proceso de formación de ribosomas, lo cual implica que los procesos de síntesis, ensamblaje y procesamiento dan como resultado final la aparición de un organelo completo. La forma regular de un nucléolo parece ser consecuencia de la

transcripción activa de genes dependiente de la RNA pol I. Por lo tanto, la inhibición con actinomicina D bloquea la formación del nucléolo (Jordan, et al., 1996).

| Genoma | Número de copias de genes ribosomales | Tamaño aproximado del genoma (pb) |
|---|---|---|
| Mitocondria de humano | 1 | $2 \times 10^4$ |
| Cloroplasto de *Nicotania tabacum* | 2 | $2 \times 10^5$ |
| *Nanoarchaeum equitans* | ~1 | $5 \times 10^5$ |
| *Mycoplasma capricolum* | 2 | $1 \times 10^6$ |
| *Escherichia coli* | 7 | $4 \times 10^6$ |
| *Methanococcus jannaschii* | 2 | $1.7 \times 10^6$ |
| *Giardia lamblia* | 60 - 300 | $1.2 \times 10^7$ |
| *Trypanosoma cruzi* | ~100 | $8.7 \times 10^7$ |
| *Neurospora crassa* | ~100 | $2 \times 10^7$ |
| *Saccharomyces cerevisiae* | ~140 | $5 \times 10^7$ |
| *Caenorhabditis elegans* | ~55 | $8 \times 10^7$ |
| *Tetrahymena termophila* | 1 | $2 \times 10^8$ |
| *Drosophila melanogaster* | 120-240 | $2 \times 10^8$ |
| *Gadus morhua* | ~50 | $3 \times 10^8$ |
| *Physarum polycephalum* | 80-280 | $5 \times 10^8$ |
| *Euglena gracilis* | 800-1000 | $2 \times 10^9$ |
| *Homo sapiens* | 300 | $3 \times 10^9$ |
| *Rattus norvergicus* | 150-170 | $3 \times 10^9$ |
| *Zea mays* | 3000-9000 | $3 \times 10^9$ |
| *Xenopus laevis* | 500-760 | $8 \times 10^9$ |

Datos tomados de Adam, 2000; Le Blancq y Adam, 1998; Graur y Li, 2000; Huber, et al., 2002.

También se ha observado la fragmentación del nucléolo cuando los genes ribosomales se redujeron a una sola copia, sugiriendo que la baja eficiencia en la síntesis de rRNA o la organización de los genes de rDNA deben influenciar fuertemente la formación del nucléolo (Oakes, et al., 1998). La identificación de una proteína parecida a la espectrina en nucléolos de anfibios también hace pensar en la posibilidad de que proteínas de citoesqueleto estuvieran participando en la organización y mantenimiento estructural del nucléolo dándole forma y soporte (Carotenuto, et al., 1997).

Experimentos en los que se privó a células de levaduras de los genes cromosomales de rDNA y se les insertó plásmido con una copia de rDNA, mostraron la formación de pequeños "mininucléolos" en lugar de un solo nucléolo bien formado (Oakes, et al., 1998). El hecho de que estas células sean viables, sugiere que ni la organización en tandem de los genes ribosomales, ni la localización cromosomal de los genes e incluso tampoco la formación de un núcleolo como se presenta en eucariontes superiores, es indispensable para

llevar a cabo la función nucleolar. Esto se corrobora al observar que en procariontes no hay nucléolo; no obstante la síntesis y maduración del rRNA tiene lugar en estas células.
Los resultados de nuestro trabajo indican que incluso en los eucariontes de divergencia más temprana existen factores que propician la conformación de un nucléolo, aunque este no tenga la estructura característica de los nucléolos descritos con anterioridad.

### I.3. *Giardia lamblia* se ha considerado un eucarionte de divergencia temprana

*Giardia lamblia* (sinónimo de *G. intestinalis*, y *G. duodenalis*) es un protista parásito anaerobio que no posee mitocondrias ni cinetoplastos, pero presenta dos núcleos, flagelos y una estructura única denominada cuerpo medio o parabasal (en Edlind and Chakraborty, 1987; Upcroft and Upcroft, 1998). Pertenece a la clase Zoomastigophora y al orden Diplomonadida y es el agente causal de severos cuadros diarreicos en humano (en Boothroyd, et al., 1987) que afectan principalmente a los niños (Boreham, 1991).
Con base en sus características bioquímicas y metabólicas, así como por estudios comparativos de sus secuencias de SSRNA, U14, fibrilarina y ATPasas, se ha considerado como el eucarionte viviente más "antiguo", esto es que, el linaje de *G. lamblia* se ramificó tempranamente en la evolución de los eucariontes (Upcroft, et al., 1987; Edlind and Chakraborty, 1987; Sogin, et al. 1989; Narcisi, *et al.*, 1998; Hilario and Gogarten, 1998). Recientemente se presentó una nueva hipótesis basada, entre otras cosas, en la existencia de eucariontes ultra pequeños, la cual sitúa al linaje de los opisthokontes como uno de los que divergió más tempranamente junto con el linaje de los excavates (Baldauf, 2003). Al primer linaje pertenecen las plantas y los animales, al segundo pertenecen protistas como los diplomonadida y los parabasalia (Baldauf, 2003). Esta nueva hipótesis debe ser tomada en cuenta cuando se propone a organismos como *G. lamblia* de divergencia temprana pero que al mismo tiempo presenta características de los grupos que se consideraban como de mayor derivación.

Los rRNAs que presentan los ribosomas de *G. lamblia* han sido motivo de gran número de estudios debido a su inusual tamaño; son más pequeños que en eucariontes y bacterias (Tabla 2). Debido a estas diferencias, las subunidades se denominan "parecidas" ("like") o SSRNA (small subunit RNA) y LSRNA (large subunit RNA).

Comparación del tamaño de las subunidades de rRNA en diferentes organismos

| Subunidad | *G. lamblia* | Levaduras | *E. coli* | Eucariontes gral. |
|---|---|---|---|---|
| SSRNA | 1300 nt | 1799 nt | 1542 nt | 1800 nt |
| 5.8S | 127-140 nt | | | 160 nt |
| LSRNA | 2300 nt | 3392 nt | 2904 nt | 3400 nt |

Tabla 2

La unidad de transcripción (rDNA) ya ha sido secuenciada en su totalidad para la cepa WB de *G. lamblia* (Healey, et al., 1990). Se sabe que es una unidad de aproximadamente 5.6kb repetida en tandem con un número de copias entre 63 y 300, y otras copias que pueden estar dispersas (Boothroyd, et al., 1987; Edlind and Chakraborty, 1987). Su organización en sentido 5'-3' presenta un ETS (al parecer no presenta NTS), SSRNA (16S like), ITS, 5.8S like, ITS y LSRNA (23S like) (figura 1) (Boothroyd, et al., 1987).

El análisis por FIGE (field inversion gel electrophoresis) muestra que *G. lamblia* tiene 5 diferentes cromosomas de tamaños aproximados de 1.6 Mb (cromosomas 1 y 2), 2.3 Mb (cromosoma 4) y 3.8 Mb (cromosoma 5) (Bernander, et al., 2001). Los genes de rRNA no están confinados a un cromosoma en particular, sino que su distribución varía dentro de las diferentes especies y cepas (Upcroft, et al. 1987).

Datos recientes han demostrado que *G. lamblia* presenta mitosomas, organelos equivalentes a las mitocondrias, pero que no llevan a cabo fosforilación oxidativa (Tovar, et al., 2003). A pesar de que varios trabajos niegan la existencia de un nucléolo morfológica y molecularmente organizado en *G. lamblia* (Narcisi, et al., 1998; Upcroft and Upcroft, 1998; Adam, 2000; Jonson, 2002), los datos generados por nuestro grupo de trabajo sugieren la existencia de una subcompartamelización nuclear de las moléculas que intervienen en la síntesis y procesamiento del rRNA (Eukaryotic mRNA processing meeting, 1999).

Comparación del tamaño de las subunidades de rRNA en diferentes organismos

| Subunidad | *G. lamblia* | Levaduras | *E. coli* | Eucariontes gral. |
|---|---|---|---|---|
| SSRNA | 1300 nt | 1799 nt | 1542 nt | 1800 nt |
| 5.8S | 127-140 nt | | | 160 nt |
| LSRNA | 2300 nt | 3392 nt | 2904 nt | 3400 nt |

Tabla 2

La unidad de transcripción (rDNA) ya ha sido secuenciada en su totalidad para la cepa WB de *G. lamblia* (Healey, et al., 1990). Se sabe que es una unidad de aproximadamente 5.6kb repetida en tandem con un número de copias entre 63 y 300, y otras copias que pueden estar dispersas (Boothroyd, et al., 1987; Edlind and Chakraborty, 1987). Su organización en sentido 5'-3' presenta un ETS (al parecer no presenta NTS), SSRNA (16S like), ITS, 5.8S like, ITS y LSRNA (23S like) (figura 1) (Boothroyd, et al., 1987).

El análisis por FIGE (field inversion gel electrophoresis) muestra que *G. lamblia* tiene 5 diferentes cromosomas de tamaños aproximados de 1.6 Mb (cromosomas 1 y 2), 2.3 Mb (cromosoma 4) y 3.8 Mb (cromosoma 5) (Bernander, et al., 2001). Los genes de rRNA no están confinados a un cromosoma en particular, sino que su distribución varía dentro de las diferentes especies y cepas (Upcroft, et al.1987).

Datos recientes han demostrado que *G. lamblia* presenta mitosomas, organelos equivalentes a las mitocondrias, pero que no llevan a cabo fosforilación oxidativa (Tovar, et al., 2003). A pesar de que varios trabajos niegan la existencia de un nucléolo morfológica y molecularmente organizado en *G. lamblia* (Narcisi, et al., 1998; Upcroft and Upcroft, 1998; Adam, 2000; Jonson, 2002), los datos generados por nuestro grupo de trabajo sugieren la existencia de una subcompartamelización nuclear de las moléculas que intervienen en la síntesis y procesamiento del rRNA (Eukaryotic mRNA processing meeting, 1999).

**I.4. El U6 snRNA participa en el corte de intrones y esta vinculado con el nucléolo**

En el nucléolo se llevan a cabo modificaciones postranscripcionales como la metilación y la pseudouridinación. Tales procesos no solo son realizados sobre los rRNAs, sino que también se efectúan sobre RNAs de bajo peso molecular, como es el caso del U3 y el U6. Se sabe que los factores necesarios para la metilación y pseudouridinación del U6 snRNA se encuentran en el nucleólo y se propone que es en este sitio donde se lleva a cabo tal proceso (Ganot, et al., 1999).

El U6 snRNA es, evolutivamente, el más conservado (tanto en tamaño como en secuencia) de los snRNAs implicados en la formación del spliceosoma (U1, U2, U4, U5 y U6) (Brow y Guthrie, 1988). A diferencia del resto de los snRNAs de splicing (corte de intrones y empalme de exones), el U6 es transcrito por la RNA pol III (Reddy, et al., 1987) y presenta en el extremo 5' un cap γ-monometil fosfato (Singh y Reddy, 1989). Se propone que el U6 snRNA está implicado directamente en la reacción para escindir los intrones de los pre-mRNAs (Newman, 1994). Tomando en cuenta que recientemente se reportó en *G. lamblia* la presencia de un gen parecido al de la ferredoxina conteniendo un intrón y que también se encontraron genes que codifican para proteínas conservadas del spliceosoma (Nixon, et al., 2002), es probable que una molécula tan conservada como el U6 pudiera estar presente en *G. lamblia*. El intrón descrito en *G. lamblia* es inusualmente pequeño (35nt) y presenta en el extremo 5' el dinucleótido CT en lugar del GT conservado en intrones de metazoarios. Sin embargo, hasta el momento no se ha reportado la presencia de ninguno de los genes que codifican para los snRNAs del splicing en esta especie. Si las funciones extras a la maduración del pre-rRNA se conservan en el nucléolo de este parásito, es posible que el U6 snRNA esté presente, y su descripción contribuya al entendimiento de los procesos que se realizan en el nucléolo de *G. lamblia*.

**I.5. La triosafosfato isomerasa es una enzima ubicua de la glucólisis y esta presente en todos los seres vivos**

El gen de la triosafosfato isomerasa (TIM o TPI) ha sido usado como marcador molecular para distinguir diferencias intraespecíficas de *G. lamblia*. Debido al debate que se ha generado con respecto a la posición filogenética de *G. lamblia* dentro de los

eucariontes, la caracterización de una molécula tan conservada como la TIM, podría servir para la discusión de los datos generados con respecto al nucléolo de este parásito.

La TIM es una enzima homodimérica que lleva a cabo la interconversión del gliceraldehído 3 fosfato (GAP) y la dihidroxiacetona fosfato (DHAP). El extenso conocimiento que se tiene de esta enzima facilita su estudio y la interpretación de los datos que se generen acerca de ella. A este respecto se conoce la secuencia de aminoácidos de la TIM de aproximadamente 80 especies y la estructura tridimensional de catorce de ellas. Además, se conoce la estructura de algunas de estas enzimas modificadas genéticamente (Borchert, *et al.*, 1993; Gopal, *et al.*, 1999; Alvarez, *et al.*, 1999; Zhang, *et al.*, 1999; Williams, *et al.*, 1999; Norledge, *et al.*, 2001), en presencia de diversos análogos de sustrato (Lolis y Petsko, 1990; Noble, *et al.*, 1991; Wierenga y Noble, 1992; Noble, *et al.*, 1993; Delboni, *et al.*, 1995; Alvarez, *et al.*, 1998; 1999; Williams, *et al.*, 1999; Zhang, *et al.*, 1999), e incluso en presencia de solventes orgánicos (Gao, *et al.*, 1999).

En adición a los conocimientos que hay sobre su estructura, se tiene bien caracterizado su mecanismo de catálisis. Esta enzima es uno de los catalizadores más eficientes que se conocen, aumentando la velocidad de la reacción $10^9$ veces (Richard, 1984).

Con respecto a la TIM de *G. lamblia* (GlTIM), solo se conoce la secuencia del gen (Mowatt *et al.*, 1994), pero nada se ha descrito con respecto a las características de la enzima. De hecho, este gen ha sido ampliamente utilizado para distinguir entre diferentes cepas de la misma especie (Li, et al., 2000). Es de hacer notar que si bien se dice que el gen de TIM de *G. lamblia* es de origen de alfa-proteobacterias (Keeling and Doolittle, 1997), nuestros resultados con respecto a la enzima muestran que tiene características peculiares, presentes algunas en eubacterias, y otras en arqueobacterias. Esta molécula también puede dar datos con respecto a las características que presenta *G. lamblia* con respecto a eucariontes y/o procariontes.

### I.6. *Trypanosoma cruzi*: un modelo para el estudio del nucléolo en eucariontes

Basados en la secuencia de la subunidad pequeña del rRNA, los kynetoplastida se ubican como un linaje de derivación temprana, solo precedidos por los diplomonadida y los parabasalia (Sogin, et al., 1989). Es de hacer notar que en este grupo se presenta un

nucléolo de forma esferoidal y con componentes fibrilares y granulares que se asemejan al de los eucariontes de derivación más tardía. Hasta el momento no existía una descripción ultraestructural detallada del nucléolo de este parásito, no obstante de ser la estructura más conspicua del núcleo de *T. cruzi*.

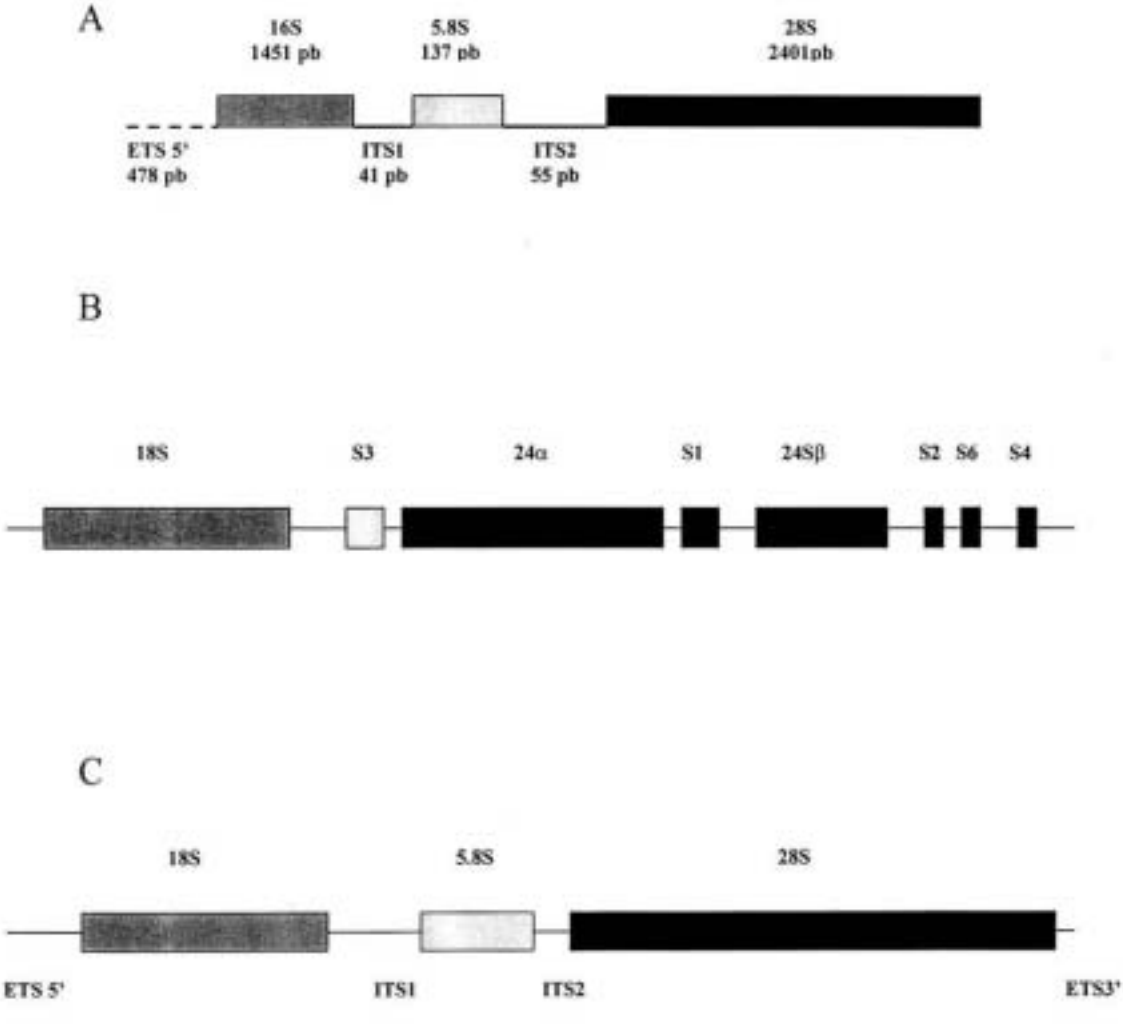


Figura 1. Arreglo de la unidad de transcripción del rDNA de A: *Giardia lamblia*, B: *Trypanosoma cruzi*, C: mamíferos.

**II. Objetivos**

II.1. Aportar datos que muestren la existencia del nucléolo en *G. lamblia* y que apoyen la presencia de esta estructura como una característica diagnóstica de los eucariontes.

II.1.1 Analizar los elementos moleculares y morfológicos que permitan reconocer el nucléolo de *G. lamblia*. Así mismo, analizar dos moléculas evolutivamente conservadas (gen del U6 snRNA y TIM) y caracterizar las propiedades mínimas que requieren para conservar su función.

II.1.2 Caracterizar ultraestructuralmente al nucléolo de *Trypanosoma cruzi* para comparar con los datos obtenidos con *G. lamblia*.

**III Material y métodos (no presentados en los manuscritos finales)**

**III.1. Aislamiento de DNA genómico**. Se partió de aproximadamente $10^8$ trofozoitos de un cultivo de 72 h en medio TYI-S-33, de la cepa WB de *G. lamblia*. Las células fueron lavadas con PBS para su posterior lisis con proteinasa K-SDS y el DNA fue extraído con fenol-cloroformo como se ha descrito con anterioridad (Upcroft y Healey, 1987), con modificaciones (López-Velázquez, et al., 1998). La concentración se midió por absorbencia a 260nm ( $1DO_{260}$= 50µg/mL DNA doble cadena) y la integridad se verificó por geles de agarosa 0.7%.

**III.2. Aislamiento de RNA total de *G. lamblia***. El aislamiento de RNA se hizo utilizando el reactivo TRIZOL (Gibco-BRL). Se partió de aproximadamente $10^8$ de trofozoitos de un cultivo de 72h en medio TYI-S-33, de la cepa WB de *G. lamblia*. Las células fueron lavadas con PBS para su posterior resuspensión en 1mL de TRIZOL a 4 °C y se homogeneizó con micropipeta. Se incubó 5 min a temperatura ambiente para promover el desensamblaje de las riboproteínas. Se adicionaron 2 mL de una mezcla 49:1 de cloroformo: alcohol isoamílico frío. Se agitó con vortex durante 2 min y se centrifugó a 10, 000 rpm/4 °C/ 15 min. Se recuperó la fase superior y se añadió un volumen igual de isopropanol frío. Se agitó suavemente por inversión del tubo y se incubó a temperatura ambiente durante 5 min. Posteriormente la muestra se centrifugó a 10, 000 rpm/4 °C/15 min. Se decantó el sobrenadante y se adicionó al botón 1 mL de etanol 75% frío. Se

resuspendió con vortex y centrifugó a 10, 000 rpm/4 °C/15 min. Se decantó el sobrenadante y el botón se secó a 37 °C para su posterior resuspensión en 200 µL de buffer TE. La concentración de RNA se calculó por espectofotometría midiendo absorbencia a 260 nm, asumiendo que 1 $DO_{260}$ = 40 µgRNA/mL. La integridad del RNA se verificó mediante geles de agarosa desnaturalizantes (fig. 2).

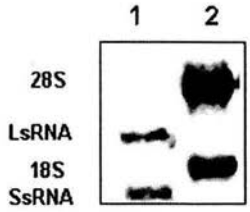


Figura 2. Gel desnaturalizante de agarosa para RNA. El carril 1 muestra el rRNA de trofozoitos de *G. lamblia* y el carril 2 muestra el rRNA de fibroblastos de humano.

**III.3. Inmunoprecipitación de RNA**. 10 µg de RNA total se disolvieron en 50 µL de buffer IPP (500mM NaCl, 10mM Tris-HCl, pH 8.0, 0.1% Nonident P-40) y se incubaron por 15 min en hielo con 100 µg de anticuerpo (anti-mGP ó anti-TMG). Se adicionaron 100µg de Proteina A-microesferas y se incubó 15 min en hielo para precipitar los anticuerpos y sus epitopes unidos. Se centrifugó a 13, 000 rpm/2 min y se tomaron las microesferas. Se hicieron 10 lavados con buffer NET2 (150 mM NaCl, 50 mM Tris-HCl, pH 7.4, 0.05% Nonident P-40). El botón se mezcló con 200 µL de agua y 200 µL de fenol:cloroformo:alcohol isoamílico ( 25:24:1 v/v) para separar el RNA de las microesferas y los anticuerpos. Posteriormente se precipitó a –70°C con NaCl 1M y etanol 100%. Se resuspendió en agua desionizada y pretratada con DEPC 0.1% (dietil pirocarbonato).

**III.4. RTPCR**. Se siguieron dos diferentes estrategias para la amplificación del transcrito del U6 snRNA. En la primera se utilizó como molde el RNA producto de la precipitación ya sea con antimGP o con antiTMG. En la segunda se utilizó directamente el RNA total. En ambos casos se utilizaron los siguientes oligonucleótidos, los cuales fueron diseñados a partir de la secuencia conservada del U6 de diferentes especies descritas con anterioridad.

5'-CAAATTGAAACGATACAGAG-'3 sentido

5'-TCATCCTTGTGCAGGGGCCA-3' antisentido

Las condiciones para la amplificación fueron como las descritas por el distribuidor del sistema de RTPCR en un solo paso (TITAN Roche). La temperatura de alineamiento fue de 42°C como se reportó para *Entamoeba histolytica* (Miranda, et al., 1996).

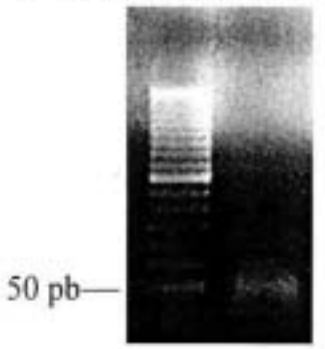


Figura 3. RTPCR a partir de RNA total de *G. lamblia*

**III.5. PCR**. Para amplificar la región conservada del gen para el U6 snRNA se usó como molde DNA genómico de trofozoitos de *G. lamblia*. Los oligonucleótidos fueron los mismos que los empleados para el RTPCR.

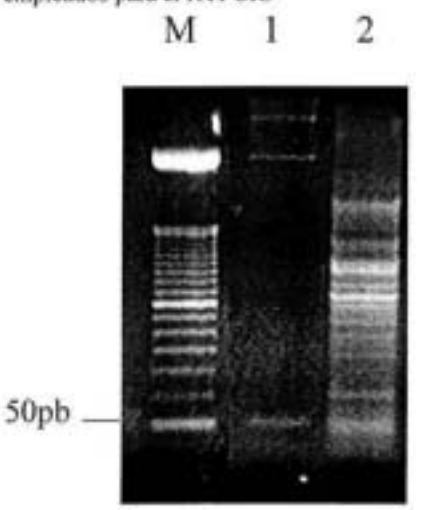


Figura 4. Gel de agarosa 2%. PCR utilizando como molde 1) clona de U6 de humano y 2) DNA genómico de trofozoitos de *G. lamblia*. M: marcador de peso molecular ladder 50pb.

**III.6. Clonación**. Los fragmentos de amplificación por PCR fueron purificados a partir de geles de agarosa 1%. Después de purificar, fueron clonados directamente al vector pCR2.1 (novagen) mediante incubación a 16°C, toda una noche con una mezcla de enzima T4 DNA ligasa y buffer de ligación 1X en presencia de ATP (New England Biolabs). La mezcla de ligación se usó para transformar células competentes *E. coli* DHα5 por choque térmico (1min/40°C). Las células fueron cultivadas en placas de agar-LB suplementadas con 50μg/mL de ampicilina. Se eligieron las colonias de color blanco y se resembraron en medio LB líquido para la posterior purificación del plásmido conteniendo el inserto de 50pb. Para corroborar la presencia del inserto, los plásmidos se sometieron a digestión enzimática con la enzima de restricción *EcoRI* que reconoce los sitios que flanquean la región de multi-inserción de pCR2.1.

**III.7. Secuenciación**. La secuenciación se llevó a cabo de forma manual por el método enzimático de Sanger y cols. (1977). A partir de aproximadamente 300ng de plásmido, se llevó a cabo un proceso de desnaturalización usando NaOH 2N y EDTA 100μM en un volumen final de 20 μL ajustado con agua desionizada. Esta mezcla se incubó a 37°C por 30 min y se precipitó con 2μL de NaOAC (acetato de sodio) 3M, pH 5.2, 100μL EtOH 100%. Se incubó durante 30 min a –70°C. Se centrifugó a 14, 000 rpm para obtener un botón que posteriormente se resuspendió en 7μL de agua desionizada. El oligonucleótido (M13 reverse ó M13 forward para el extremo 3' y 5' respectivamente) se alineó incubando a 65°C durante 7 min y 30 min a 37°C. La síntesis de la cadena de DNA se hizo con la enzima Thermo Sequenase (8 unidades) (USB Corp.) y adicionando dATP con $^{32}P$. Para detener la síntesis, la mezcla se incubó 15 min a 37°C en 4 tubos diferentes con ddGTP, ddTTP, ddCTP y ddATP respectivamente. La reacción se detiene usando EDTA e incubando 2 min a 80°C. Las muestras se corrieron en un gel de secuenciación de acrilamida 16%. Después de correr el gel durante aproximadamente 2h, se secó por vacío, y se puso una placa fotográfica expuesta al mismo durante toda la noche a –70°C. La placa se reveló y se procedió a la lectura manual de la secuencia (figura 5).

**III.8. Alineamiento y comparación de secuencias**. Se comparó la secuencia encontrada en el gDNA contra los datos recopilados en el proyecto del genoma *de Giardia lamblia* y

se identificó una región parecida al gen del U6. Para alineamientos globales de secuencias se utilizó el Clustal W (Combet, et al., 2000). Para alineamientos locales se utilizó FASTA3 (Pearson, et al., 1988).

## IV. Resultados y Discusión (no presentados en los manuscritos para publicación)

### IV.1. El genoma de *G. lamblia* presenta regiones conservadas del gen del U6 snRNA.

El gen de U6 snRNA tiene una longitud de entre 100 a 120 nt, dependiendo de la especie. Con el uso de los oligonucleótidos diseñados a partir de la región conservada de 50 nt del gen de U6, se logró amplificar un fragmento equivalente en tamaño, tanto a partir de gDNA como de RNA total (figuras 3 y 4). De acuerdo con trabajos previos, estos resultados son un indicio de la presencia del gen y su transcrito en el organismo (Tani y Ohshima, 1991; Miranda, et al., 1996). La secuencia nucleotídica de este fragmento correspondió a la región conservada del U6 snRNA (figura 5), la cual es la más conservada en todas las especies y se le atribuye la actividad nucleolítica del U6 en el spliceosoma (Brow y Guthrie , 1988). Al comparar la secuencia nucleotídica contra el genoma de *G. lamblia*, se obtuvo una secuencia ( NJ3094_A.r) que presenta 3 de las regiones altamente conservadas en el gen de U6 . La tabla 3 muestra estas regiones y su comparación con las secuencias consenso. Los datos sugieren la presencia del gen del U6 snRNA en el genoma de *G. lamblia* . Esto nos da la pauta para sugerir que la maquinaria de splicing, o al menos algunos elementos de ella, podría considerarse como una característica diagnostica de los eucariontes.

| Secuencia consenso de elementos conservados del U6 snRNA | Secuencia en *G. lamblia* |
|---|---|
| AGATTAGCATGG<br>ACAGAGA<br>AGC | *AGATTAGCAG*<br>ACAGAGA<br>AGC |

Tabla 3. Regiones conservadas del gen de U6 snRNA de *G. lamblia*


**5' TCATCCTTGTGCAGGGGCCATGCTA**
**ATCTTCTCTGTATCGTTTCAATTTG 3'**

Figura 5. Secuencia de la región conservada del gen de U6 snRNA de *G. lamblia*.

Cabe señalar que esta región conservada no pudo ser amplificada a partir de los ensayos de inmunoprecipitación contra la región de cap, lo cual hace suponer que el transcrito del U6 en *G. lamblia* no presenta una región cap como las descritas para otros U6 en el extremo 5'.

**IV.2. El spliceosoma en *G. lamblia* podría ser similar al splicing mayor.**

Al confrontar mediante BLASTN (ver. 2.2.2) la secuencia obtenida en este trabajo contra la base de datos del proyecto del genoma de *G. lamblia* (www.mbl.edu/Giardia ), se obtuvo la secuencia NJ3094_A.r (Stephen, et al., 1997). La secuencia del genoma de *G. lamblia* presenta un porcentaje de identidad de 38.71 % contra el gen de U6 de *T. brucei*, 37.77 % contra el de humano, 38.92 % contra el U6atac, y de 37.3 % contra el 87U6. Existen formas alternativas de genes de U6 en humano (U6atac, 87U6) que se propone intervienen de forma alternativa en el splicing, o que están relacionados con el procesamiento de intrones de secuencias diferentes a la mayoría (Wieben, et al., 1991; Tichelaar et al., 1998).

Tomando en cuenta que el U6atac exhibe un 40% de identidad con el U6 de humano (Woan-Yuh y Steitz, 1996), nuestros datos sugieren que la secuencia encontrada en *G. lamblia* se encuentra dentro de este intervalo con respecto a las secuencias de comparación.

El alineamiento local reconoce de 3 a 5 sitios conservados al comparar contra las secuencias del gen de U6 de *Thermus thermophila*, *Trypanosoma brucei*, *Entamoeba histolytica*, *Caenorabditis elegans*, *Schizosacharomices pombe*, *Sacharomices cerevisiae*, *Drosophila melanogaster* y humano (constitutivo, 87U6 y U6atac). El genoma de *G. lamblia* presenta 23nt de los 34nt que en el gen de U6 de humano participan en la formación del asa I y II; regiones que se sabe interactúan con el U4. *G. lamblia* también presenta la región ACA de interacción con los intrones del splicing mayor, a diferencia de la secuencia AAGGA de interacción con los intrones tipo AT-AC. Nuestros datos tienden a sugerir la presencia de una maquinaria de splicing parecida a la que se presenta en el splicing mayor. No obstante hasta no tener la secuencia completa del gen aislado directamente del genoma de *G. lamblia* y de realizar ensayos de complementación con este gen, no podremos confirmar tales aseveraciones. También es factible que existiera más de una secuencia codificante para variantes del gen de U6, como sucede en humano, por lo que debemos seguir estos estudios para determinar si esto es cierto. Dado que la secuencia encontrada en el genoma de *G. lamblia* no esta completa y que no se encontraron las regiones correspondientes al consenso para el extremo 3' y 5' del gen de U6, no se puede asegurar aún que este sea el U6. Es muy probable que el proyecto del genoma de *Giardia* terminado y depurado nos permita identificar de manera correcta la región que contiene este gen.

## V. Referencias


Adam RD (2000). The *Giardia lamblia* genome. Int. J. Parasitol., 30: 475-84.

Stephen F, Madden L, Schäffer A, Zhang J, Zhang Z, Miller W, Lipman D. (1997). Gapped BLAST and PSI-BLAST: a new generation of protein database search programs. Nucleic Acids Res. 25: 3389-3402.

Alvarez M, Zeelen JP, Mainfroid V, Rentier-Delrue F, Martial JA, Wyns L, Wierenga RK, Maes D. (1998) Triose-phosphate isomerase (TIM) of the psychrophilic bacterium *Vibrio marinus*. Kinetic and structural properties J. Biol. Chem. 273:2199-2206.

Alvarez M, Wouters J, Maes D, Mainfroid V, Rentier-Delrue F, Wyns L, Depiereux E, Martial JA. (1999) Lys13 plays a crucial role in the functional adaptation of the thermophilic triose-phosphate isomerase from *Bacillus stearothermophilus* to high temperatures. J. Biol. Chem. 274:19181-19187.

Baldauf SL (2003).The deep roots of eukaryotes. *Science*, 300: 1703-6.

Bernander R, Palm JED, Svärd SG. (2001) Genome ploidy in different stages of the *Giardia lamblia* life cycle.Cellular Microbiol., 3(1), 55-62.

Boothroyd J, Wang A, Campbell DA, Wuang ChC, (1987) An unusual compact ribosomal DNA repeat in the protozoan *Giardia lamblia*. Nucleic Acids Res., 15: 10, 4065-84.

Borchert, TV., Pratt, K., Zeelen, JP., Callens, M., Noble, ME., Opperdoes, FR., Michels, PA., Wierenga, RK. (1993). Overexpression of trypanosomal triosephosphate isomerase in *Escherichia coli* and characterisation of a dimer-interface mutant. Eur J Biochem. 211:703-10.

Boreham PFL (1991). Giardiasis and its control. Pharm. J. 234:271-74.

Brow DA, Guthrie C (1988). Spliceosomal RNA U6 is remarkably conserved from yeast to mammals. Nature, 334: 213-218.

Carotenuto R, Maturi G, Infante V, Capriglione T, Petrucci TC, Campanella C (1997). A novel protein cross-reactin with antibodies against spectrin is located in the nucleoli of amphibian oocytes. J. Cell Sci., 110, 2683-2690.

Combet C, Blanchet C, Geurjon C, Deléage G (2000). NPS@: network protein sequence analysis. Trends Biochem Sci., 25:3, 147-150.

Delboni LF, Mande SC, Rentier-Delrue F, Mainfroid V, Turley S, Vellieux FM, Martial JA, Hol WG. (1995). Crystal structure of recombinant triosephosphate isomerase from *Bacillus stearothermophilus*. An analysis of potential thermostability factors in six isomerases with known three-dimensional structures points to the importance of hydrophobic interactions. Protein Sci. 1995 Dec;4(12):2594-604

Ganot P, Jády B, Bortolin M, Darzaco X, Kiss T (1999). Nucleolar factors direct the 2'-O-Ribose methylation and pseudouridylation of U6 spliceosomal RNA. Mol. Cell. Biol. 19: 6906-6917.

Gao XG, Maldonado E., Pérez-Montfort R, Garza-Ramos G, Tuena de Gómez-Puyou M, Gómez-Puyou A, Rodriguez-Romero A. (1999) Crystal structure of triosephosphate isomerase from *Trypanosoma cruzi* in hexane. Proc. Natl. Acad. Sci. USA. 96:10062-10067.

Gopal B, Ray SS, Gokhale RS, Balaram H, Murthy MRN, Balaram P. (1999). Cavity-creating mutation at the dimer interface of *Plasmodium falciparum* triosephosphate isomerase: restoration of stability by disulfide cross-linking of subunits. Biochemistry. 38:478-486.

Graur D, Li WH. **Fundamentals of Molecular Evolution**. 2nd ed. Sinauer Associates Inc., USA, 2000, 481 pp.

Healey A, Mitchell R, Upcroft JA, Boreham PFL, Upcroft P, (1990) Complete nucleotide sequence of the ribosomal RNA tandem repeat unit from *Giardia intestinalis*. Nucleic Acids Res. 18: 13, 4006.

Hilario E, Gogarten JP (1998). The prokaryote-to-eukaryote transition reflected in the evolution of the V/F/A-ATPase catalytic and proteolipid subunits. *J. Mol. Evol.*, 46; 703-15.

Huber H, Hohn MJ, Rachel R, Fuchs T, Wimmer VC, Stetter KO. (2002). A new phylum of Archaea represented by nanosized hyperthermophilic symbiont. Nature, 2;417(6884):63-67.

Jiménez-García LF, Ramos P, Chávez B, López Velázquez G, Zavala- Padilla G. (1999). Nucleoli are present in *Giardia lamblia*. Eukaryotic mRNA processing meeting, 25-29 August, 1999, Cold Spring Harbor Laboratory, NY, USA.

Jonson PJ (2002). Spliceosomal introns in a deep-branching eukaryote: The splice of life. Proc Natl Acad Sci U S A. 99: 3359-61.

Jordan P, Mannervivik M, Tora L, Carmo-Fonseca M. (1996). In vivo evidence that TATA-binding protein/SL1 colocalizes with UBF and RNA polymerase I when rRNA synthesis is either active or inactive. J. Cell Biol., 133:225-234.

Keeling PJ, Doolittle WF. (1997). Evidence that eukaryotic triosephosphate isomerase is of alpha-proteobacterial origin. Proc Natl Acad Sci USA, 94:1270-1275.

Le Blancq SM, Adam RD. (1998). Structural basis of karyotype heterogeneity in *Giardia lamblia* . Mol. Biochem. Parasitol, 97: 199-208.

Li JH, Lu SQ, Zhang YP, Wang FY, Wen JF. (2000). Molecular phylogeny of *Giardia lamblia* based on triose phosphate isomerase (tim) gene sequence. Zhongguo Ji Sheng Chong Xue Yu Ji Sheng Chong Bing Za Zhi. 18:141-145.

Lolis E, Petsko GA. (1990). Crystallographic analysis of the complex between triosephosphate isomerase and 2-phosphoglycolate at 2.5-A resolution: implications for catalysis. Biochemistry. 29:6619-6625.

López-Velázquez, G., Segura-Valdez, M.A., Alcántara-Ortigoza, M.A., Jiménez-García L.F., 1998. Localization of intranuclear RNA by electron microscopy *in situ* hybridization using a genomic DNA probe. Arch. Med. Res. 29, 185-190.

Miranda R, Salgado LM, Sánchez-López R, Alagón A, Lizardi PM (1996). Identification and analysis of the u6 small nuclear RNA gene from *Entamoeba histolytica*. Gene, 180: 37-42.

Narcisi EM, Glover VC, Fechheimer M, (1998) Fibrillarin, a conserved pre-ribosomal RNA processing protein of *Giardia*. J. Euk. Microbiol. 45: 1, 105-111.

Newman A (1994). Activity in the spliceosoma. Curr. Biol., 4:462-464.

Noble ME, Wierenga RW, Lamberi AM, Opperdoes FR, Thunisen AMWH, Kalk KH, Groendijk m, Hol WGJ. (1991). The adaptability of the active site of trypanosomal triosephosphate isomerase as observed in the crystal structures of three different complexes Proteins Struct. Funct. Genet. 10:311-326.

Noble ME, Zeelen JP, Wierenga RK. (1993) Structures of the "open" and "closed" state of trypanosomal triosephosphate isomerase, as observed in a new crystal form: implications for the reaction mechanism. Proteins: Struct. Funct. Genet. 16:311-326.

Norledge BV, Lambeir AM, Agabyan RA, Rottmann A, Fernandez AM, Filimonov VV, Peter MB, Wierenga RK. (2001). Modeling, mutagenesis, and structural studies on the fully conserved phosphate-binding loop (loop 8) of triosephosphate isomerase: toward a new substrate specificity. Proteins: Struc. Function Genet. 42:383-389.

Oakes M, Aris JP, Brockenbrough, Wai H, Vu L, Nomura M. (1998). Mutational analysis of the structure and localization of the nucleolus in the yeast *Saccharomyces cerevisiae*. J. Cell Biol., 143:23-34.

Pearson WR, Lipman DJ (1988). Improved tools for biological sequence comparison. Proc Natl Acad Sci U S A. 85, 2444-2448.

Reddy R, Henning D, Das G, Harless M, Wright D (1987). The capped U6 small nuclear RNA is transcribed by RNA polymerase III. J. Biol. Chem. 262, 75-81.

Richard JP. (1984) Acid-base catalysis of the elimination and isomerization ractions of triose phosphates J. Am. Chem. Soc. 106:4926-4936.

Sanger F, Nicklen S, Coulson AR (1977). DNA sequencing with chain-terminating inhibitors. Proc. Natl. Acad. Sci. USA, 74 (12): 5463-5467.

Singh R, Reddy R. (1989). γ-monomethyl phosphate: a cap structure in spliceosomal U6 small nuclear RNA. Proc. Natl. Acad. Sci. USA, 86:8280-8283.

Sogin ML, Gunderson JH, Elwood HJ, Alonso RA, Peattie DA, (1989) Phylogenetic meaning of the kingdom concept: an unusual ribosomal RNA from *Giardia lamblia*. Science , 6, 75-77.

Tichelaar JW, Wieben ED, Reddy R, Vrabel A, Camacho P (1998). In vivo Expression of a variant human U6 RNA from a unique, internal promoter. Biochemistry, 37, 12943-12951.

Tovar J, Leon-Avila G, Sanchez LB, Sutak R, Tachezy J, Van Der Giezen M, Hernández M, Müller M, Lucocq JM. Mitochondrial remnant organelles of *Giardia* function in iron-sulphur protein maturation. Nature. 2003 426:172-176.

Upcroft JA, Healey A, Mitchell R, Boreham PFL, Upcroft P, (1990) Antigen expression from the ribosomal DNA repeat unit of *Giardia intestinalis*. Nucleic Acids Res. 18: 23, 7077-81.

Upcroft P, Healey A (1987). Rapid and efficient method for cloning of blunt-ended DNA fragments. Gene, 51: 69-75.

Wieben ED, Vrabel AM, Holicky EL, Klisak I, Sparkes RS, Stanford DR. (1991). A U6 snRNA gene with an internal promoter juxtaposed to an snRNP protein sequence within an intron of a human protein gene. Nucleic Acids Res., 19: 2869-2874.

Wierenga RK, Noble ME. Comparison of the refined crystal structures of liganded and unliganded chicken, yeast and trypanosomal triosephosphate isomerase. (1992) J. Mol. Biol. 224:1115-1126.

Williams JC, Zeelen JP, Neubauer G, Vriend G, Backmann J, Michels PA, Lambeir AM, Wierenga RK. (1999). Structural and mutagenesis studies of Leishmania triosephosphate isomerase: a point mutation can convert a mesophilic enzyme into a superstable enzyme without losing catalytic power. Protein Eng. 12:243-250.

Woan-Yuh T, Steitz JA (1996). Higly diverged U4 andU6 small nuclear RNAs required for splicing rare AT-AC introns. Science, 273, 1824-1832.

Zhang Z, Komives EA, Sugio S, Blacklow SC, Narayana N, Xuong NH, Stock AM, Petsko GA, Ringe D. (1999). The role of water in the catalytic efficiency of triosephosphate isomerase. Biochemistry 38:4389-4397.

**Apéndice**

Manuscritos para publicación de los resultados.

1. Nucleolus is present in *Giardia lamblia*
2. An unusual triosephosphate isomerase from the early divergent eukaryote *Giardia lamblia*
3. Ultrastructural analysis of the nucleolus of *Trypanosoma cruzi*

# Nucleolus is present in *Giardia lamblia*

Abstract

The nucleolus is the major nuclear ribonucleoprotein structure, and is the site where synthesis and processing of pre-rRNA and ribosome assembly take place. To see if this organelle was already present in the first eukaryotes, we used electron microscopy to analyze the nuclei of the protist *Giardia lamblia*, a human parasite that causes diarrhea and is considered one of the earliest eukaryote. Both nuclei in cultured trophozoites of *G. lamblia* display a peripheral fibro-granular structure that is also present in cysts. This structure is composed of ribonucleoproteins and contains nucleolar organizer silver staining proteins, the nucleolar protein fibrillarin and ribosomal RNA. We concluded that nucleoli are present in *G. lamblia* and suggest that ribosome biogenesis took place in an intranuclear compartment in earliest eukaryotes.

*Giardia lamblia* is a diplomonad protist that causes diarrhea in humans and other vertebrates (Adam, 1991; Boreham, 1991). In addition to this inherent importance in human health, this microorganism has attracted attention of biologists because molecular analyses shows a very early separation from the main branch of eukaryote evolution (Sogin, et al. 1989, Belhadri, 1995). Comparative analyses from ribosomal genes sequence, nucleolar proteins as fibrillarin and ATPases, indicate that *G. lamblia* belongs to a very early branch during eukaryote evolution (Sogin, et al. 1989; Narcisi, et al. 1998 ; Hilario and Gogarten, 1998). Since its first description in 1681, *G. lamblia* has been the subject of numerous studies contributing to its biology (Adam, 1991). Recently , most studies are devoted to understand its cell and molecular biology (Seshadri, et al., 2003; Vanacova, et al., 2003). As a result, *G. lamblia* is considered to be an early diverging organism that represents one of the deepest branches of eukarya. The presence of a nuclear structure defines *G. lamblia* as an eukaryote, although prokaryote biochemical and molecular characteristics are also observed (Mowatt et al., 1994). At the cellular level this unicellular protist has two identical nuclei where 5 chromosomes have been described. A not well defined endomembrane system of protein modification, sorting and transport is also observed containing structures resembling endoplasmic reticullum and vesicules. Cytoskeleton elements are present as a flagellar apparatus and a ventral adhesive disc. On the other hand, no mitochondria, but mitosomes lacking oxidative phosphorilation, peroxisomes, glycosomes or hydrogenosomes have been described (Tovar, et al., 2003 ).

*G. lamblia* have two nuclei with identical DNA amount and both are transcriptionally active (Kabnick and Peattie, 1990). The nuclear envelope does not break down during cell division. In addition to the absence of many organelles, *G. lamblia* has been also considered not to have nucleoli (Adam, 2000; Narcisi et al., 1998), the main site in the eukaryote cell were synthesis and processing of pre-rRNA and ribosome assembly takes place (Carmo-Fonseca, et al., 2000). Many nucleolar materials have been found in *G. lamblia*, but light microscopy cytochemistry as immunofluorescence and *in situ* hybridization have failed to demonstrate the presence of a nucleolus (Kabnick and Peattie,

1990). Because the small size of *G. lamblia* nuclei (mean size is about 2 μm long) (Adam, 1991), it is not possible to visualize intranunclear structures with the resolution of light microscopy. Therefore, we used several electron microscopy techniques to visualize nucleolar material. First we performed silver staining for NOR at the light microscopy (Goodpasture and Bloom, 1975). Highly impregnated peripheral dots measuring about 0.3 μm by 0.8 μm within the nuclei of a culture of *G. lamblia* trophozoites were observed (morphometric). Then we analyze nuclear structure with standard electron microscopy and by using cryofixation and cryosubstitution to better preserve fine details (Vázquez-Nin and Echeverría, 2000). Figure 1.A illustrates samples after this procedure, where two nuclei display an irregular peripheral fibrogranular dense zone. A preferential method (Bernhard, 1969) supports the ribonucleoprotein (RNP) composition of this zone (Fig. 1.B). Ultrastructural silver staining was then used to test the nucleolar proteins in this structure. A peripheral zone in both nuclei was also highly impregnated (Fig. 1.C) which is negative for DNA (Fig. 1.D) as seen with immunoelectron microscopy using primary monoclonal antibodies followed by secondary antibodies coupled to colloidal gold particles. A peripheral zone was also intensively labeled after immunoelectron microscopy using antibodies to nucleolar protein fibrillarin (Fig. 1.E) and after ultrastructural *in situ* hybridization using probes to detect rRNA (Fig. 1.F). Taken together our results strongly support the presence of a 0.3 to 0.5 μm intranuclear ribonucleoprotein peripheral fibrogranular structure enriched on silver staining proteins, fibrillarin and rRNA that we identified as authentic nucleoli within both nuclei of *G. lamblia* trophozoites. 3D computational assisted reconstruction showed the disposition of this structure in one of the nuclei from *G. lamblia* trophozoite (Fig. 2). Because of molecular studies indicating that *G. lamblia* belongs to one of the deepest branches of eukaryote evolution, we suggest that a feature of earliest eukaryotes on earth was the segregation and compartmentalization of ribosome biogenesis machinery within a nuclear territory containing the basic elements of a nucleolus. Ribosomal genes in *G. lamblia* therefore, although having a prokaryote-like organization, should then have the capability to organize a nucleolus. *G. lamblia* may be a good model to search for the basic elements of the nucleolar organizer region (NOR).

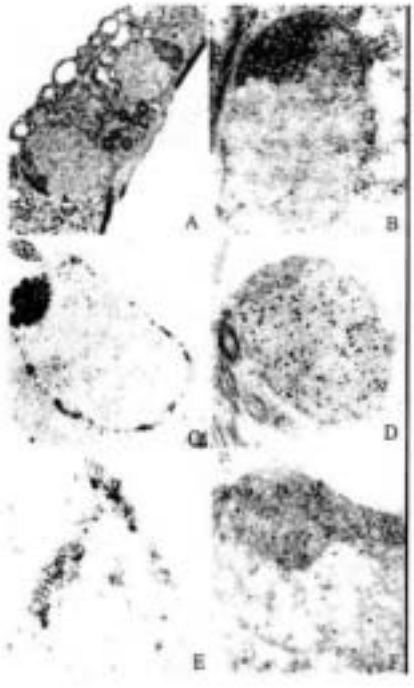


Figure 1. *In situ* distribution of the molecules related to rRNA processing in *G. lamblia* nucleus. A. Cryofixation, B. Ribonucleoprotein staining, C. AgNOR staining, D. Anti-DNA, E. Anti-fibrillarin, and F. rRNA hybridization.

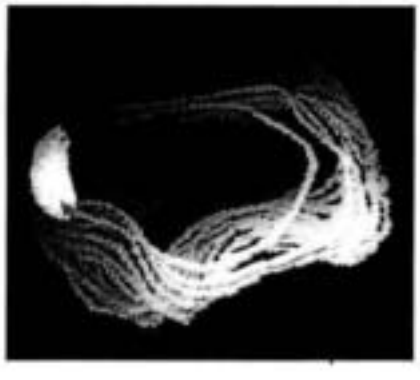

Figure 2. Computational 3D reconstruction of a nucleus from *G. lamblia* trophozoite. Nucleolus: yellow; Nuclear envelope: orange.

## References


Adam RD (1991). The biology of *Giardia* spp. Microbiol. Rev, 4, 706-32.

Adam RD (2000). The *Giardia lamblia* genome. Int. J. Parasitol. 30: 475-484.

Belhadri A. (1995). Presence of centrin in the human parasite *Giardia*: a fhurther indication of its ubiquity in eukaryotes. Biochem. Biophys. Res. Comm. 214:2, 597-601.
Bernhard W (1969) A new staining procedure for electron microscopical cytology, *J Ultrastruct Res*, 27:250-258.

Boreham PFL (1991). Giardiasis and its control. Pharm J, 234, 271-274.

Carmo-Fonseca M, Mendes-Soares L, Campos I (2000). To be or not to be in the nucleolus. *Nature Cell Biol.*, 2: E107-E112.

Hilario E, Gogarten JP (1998). The prokaryote-to-eukaryote transition reflected in the evolution of the V/F/A-ATPase catalytic and proteolipid subunits. J. Mol. Evol., 46, 703-715.

Kabnick KS, Peattie DA (1990). *In situ* analyses reveal that the two nuclei of *Giardia lamblia* are equivalent. J. Cell Sci.,95: 353-60.

Mowatt MR, Weinbach EC, Howard TC, Nash TE (1994). Complementation of an *Escherichia coli* Glycolisis Mutant by *Giardia lamblia* Triosephosphate Isomerase. Exp. Parasitol. 78, 85-92.

Narcisi EM, Glover CVC, Fechheimer M (1998). Fibrillarin, A conserved pre-ribosomal RNA processing protein of *Giardia*. J Euk Microbiol, 45: 105-11.

Olson MOJ, Dundr M, Szebeni A (2000). The nucleolus: and old factory with unexpected capabilities. *Trends Cell Biol.* 10; 189-91.

Seshadri V, McArthur AG, Sogin ML, Adam RD. (2003). *Giardia lamblia* RNA polymerase II:amanitin-resistant transcription. Biol Chem, 278(30):27804-27810.

Sogin M.L., Gunderson J.H. Elwood H.J., Alonso R.A. and Peattie D.A.(1989). Phylogenetic Meaning of the Kingdom Concept: An Unusual Ribosomal RNA from *Giardia lamblia*. *Science*, 243, 75-77.

Tovar J, Leon-Avila G, Sanchez LB, Sutak R, Tachezy J, Van Der Giezen M, Hernández M, Müller M, Lucocq JM. Mitochondrial remnant organelles of *Giardia* function in iron-sulphur protein maturation. Nature. 2003 426:172-176.

Vanacova S, Liston DR, Tachezy J, Johnson PJ. (2003). Molecular Biology of the amitochondriate parasites, Giardia intestinalis, Entamoeba histolytica, and Trichomonas vaginalis. Int J Parasitol. 33(3):235-255.

Vázquez-Nin GH, Echeverria OM (2000) *Introducción a la microscopia electrónica aplicada a las ciencias biológicas*. Universidad Nacional Autónoma de México-Fondo de Cultura Económica, pp.168.

PROTEINS: Structure, Function, and Bioinformatics 55:824–834 (2004)

# An Unusual Triosephosphate Isomerase from the Early Divergent Eukaryote *Giardia lamblia*

**Gabriel López-Velázquez,[1]* Dora Molina-Ortiz,[1] Nallely Cabrera,[2] Gloria Hernández-Alcántara,[1] Jorge Peon-Peralta,[3] Lilian Yépez-Mulia,[4] Ruy Pérez-Montfort,[2] and Horacio Reyes-Vivas[1]***

[1]*Laboratorio de Bioquímica-Genética, Instituto Nacional de Pediatría, México, D.F. México*
[2]*Instituto de Fisiología Celular, Universidad Nacional Autónoma de México, México, D.F. México*
[3]*Instituto de Química, Universidad Nacional Autónoma de México, México, D.F. México*
[4]*UIMEIP-Pediatría, Centro Médico Nacional-Siglo XXI, IMSS*

*ABSTRACT* **Recombinant triosephosphate isomerase from the parasite *Giardia lamblia* (GlTIM) was characterized and immunolocalized. The enzyme is distributed uniformly throughout the cytoplasm. Size exclusion chromatography of the purified enzyme showed two peaks with molecular weights of 108 and 55 kDa. Under reducing conditions, only the 55-kDa protein was detected. In denaturing gel electrophoresis without dithiothreitol, the enzyme showed two bands with molecular weights of 28 and 50 kDa; with dithiotretitol, only the 28-kDa protein was observed. These data indicate that GlTIM may exist as a tetramer or a dimer and that, in the former, the two dimers are covalently linked by disulfide bonds. The kinetics of the dimer were similar to those of other TIMs. The tetramer exhibited half of the $k_{cat}$ of the dimer without changes in the Km. Studies on the thermal stability and the apparent association constants between monomers showed that the tetramer was slightly more stable than the dimer. This finding suggests the oligomerization is not related to enzyme thermostability as in *Thermotoga maritima*. Instead, it could be that oligomerization is related to the regulation of catalytic activity in different states of the life cycle of this mesophilic parasite. Proteins 2004;55: 824–834.** © 2004 Wiley-Liss, Inc.



**Key words: glycolysis; giardiasis; protein purification; oligomerization state; disulfides**

## INTRODUCTION

The protozoan parasite *Giardia lamblia* merits extensive studies for several reasons. From the evolutionary point of view, *G. lamblia* has been considered a rather remarkable organism because its morphological, metabolic, and molecular features correspond to those of one of the earliest branching lineages of eukaryotes.[1–5] Indeed, the G+C content, gene complementation, and rRNA subunits of *G. lamblia* are markedly similar to those of prokaryotic organisms. In addition, the parasite is the causative agent of human giardiasis, a worldwide disease that affects millions of people, in particular children.[6] Although metronidazole is effective in giardiasis,[7] it exerts strong side effects in the host,[8] and there is clear evidence that strains of *G. lamblia* resistant to metronidazole are now existent.[9] This finding underlines the need for developing drugs that are effective against giardiasis. In this regard, it is noted that an additional feature of *G. lamblia* is that it lacks mitochondria and oxidative phosphorylation.[10] Thus, in *G. lamblia*, the main source of ATP is the glycolytic pathway.[11] This finding suggests that the enzymes of glycolysis could be potential targets for drug design. The nucleotide sequence of the triosephosphate isomerase gene from *G. lamblia* has been previously reported.[12] However, there are no data on the kinetics and structure of triosephosphate isomerase from *G. lamblia*. Therefore, because of its importance in the evolutionary processes and its potential as a target for drug design, we characterized triosephosphate isomerase from *G. lamblia* (GlTIM) and also determined its distribution within the parasite.

TIM is a ubiquitous glycolytic enzyme that catalyzes the reversible isomerization between (R)-glyceraldehyde 3-phosphate (GAP) and dihydroxyacetone phosphate (DHAP). The kinetics and energetics of the catalytic reaction are well established,[13–16] and the three-dimensional (3D) structure of the enzyme from 13 different species has been determined. The active site residues of all known TIMs are located in the central region of the α/β-barrel and belong to the same main-chain. Most TIMs so far described are homodimers in which each of the two monomers exhibits an α/β-barrel structure. However, some TIMs from hyperthermophilic organisms have a different quaternary structure, which apparently is related to their thermal stability. For example, TIMs from *Pyrococcus woesei*[17,18] and *Methanothermus fervidus*[19] are tetrameric enzymes. In *Thermotoga neapolitana* and *T. maritima*, the enzyme is a tetramer fused with a phosphoglycerate kinase.[20,21] TIM from *T. maritima* was separated from phosphoglycerate kinase and crystallized.[21] The modified TIM was a tetramer in which two dimers were in close contact through hydrophobic and polar residues. However,

Grant sponsor: Consejo Nacional de Ciencia y Tecnología, México; Grant number: J37071-B.

*Correspondence to: Gabriel López-Velázquez and Horacio Reyes-Vivas. Laboratorio de Bioquímica-Genética, Instituto Nacional de Pediatría, Apartado Postal 04530, México, D.F. México. E-mail: hreyesvivas@yahoo.com.mx.

Received 7 August 2003; Accepted 11 December 2003

Published online 1 April 2004 in Wiley InterScience (www.interscience.wiley.com). DOI: 10.1002/prot.20097

it is relevant to this work that the dimers of *T. maritima* were joined through two disulfide bridges, between Cys 142 of each monomer. Our studies on GlTIM show that it is an enzyme with characteristics different from those of TIMs from other mesophilic organisms.

## MATERIALS AND METHODS

### Parasites

Trophozoites of *G. lamblia* WB strain were cultured in TYI-S-33 as previously described.[22] Cultures were grown at 37°C for 72 h to semiconfluence and washed with phosphate buffered saline (PBS), pH 7.3.

### Amplification of Triosephosphate Isomerase Gene From *Giardia lamblia*

Genomic DNA from *G. lamblia* trophozoites (WB strain) was purified by the phenol-chloroform method with slight modifications.[23] The polymerase chain reaction (PCR) conditions were those described by Gibco-BRL (Taq polymerase supplier) using the following oligonucleotides: sense 5′-AATAACATATGCCTGCTCGTC-3′ and antisense 5′-CCAGGATCCTATGTACGGG-3′, which contain *Nde*I and *Bam*HI restriction sites at the 5′ end, respectively. The reaction mixture contained 400 ng of gDNA, 1.5 mM $MgCl_2$, 0.8 mM of dNTP, and 2.5 units of Taq Polymerase (Gibco-BRL). Amplification was performed by using 30 cycles of 1 min at 94°C, 1 min at 57°C, and 1 min at 72°C.

### Cloning of the GlTIM Gene and Sequence Analysis

The amplified DNA fragment was purified by electrophoresis using an extraction kit (Concert; Gibco-BRL) and cloned into the pCR2.1 vector, as recommended (Novagen). *E. coli* TOP10 competent cells were transformed for cloning. The cloned fragment was subcloned into the pET3a vector after digestion with *Nde*I and *Bam*HI enzymes and used to transform *E. coli* TOP10 competent cells. Enzyme restriction assays and electrophoresis were performed to confirm the correct fragment insertion into the vector.

The plasmid from positive clones was purified by using an extraction plasmid kit (Concert; Gibco-BRL) and sequenced by the enzymatic method with an automatic sequencer. A clone named 13* showed the correct sequence and orientation of the gene of *G. lamblia* TIM. This was used for the production of wild-type recombinant GlTIM.

### Overexpression of GlTIM in *E. coli*

The plasmid from clone 13* was extracted and used to transform competent *E. coli* BL21(DE3)pLys cells. BL21 cells contain the gene codifying for the T7 RNA pol needed for expression of the recombinant enzyme. The transformed cells were grown in Luria-Bertani medium with 100 μg/mL ampicillin at 37°C to an $A_{600nm}$ of 0.2–0.5. To induce overexpression, 0.4 mM isopropyl β-D-thiogalactopyranoside was added, and growth was continued overnight at 30°C.

### Purification of Recombinant GlTIM

Transformed bacteria from 1 L culture were suspended in 80 mL of a buffer containing 25 mM Tris, 1 mM EDTA, 0.2 mM phenylmethylsulfonyl fluoride, pH 7.9. The cells were disrupted by sonication at 4°C, six cycles of 45 s with 75 s of resting intervals. The sonicate was centrifuged at 45,000 rpm for 1 h, and the supernatant was taken to 45% saturation ammonium sulfate. The suspension was allowed to stand for 3 h at 4°C and thereafter was centrifuged at 10,000 rpm for 30 min. The pellet was discarded, and the concentration of ammonium sulfate in the supernatant was increased to 75% saturation. The suspension was incubated at 4°C overnight. It was then centrifuged at 10,000 rpm for 30 min, and the supernatant was discarded. The pellet was suspended in 5 mL of a buffer containing 25 mM Tris, 1 mM EDTA, 1 mM $NaN_3$, pH 8, and filtered (0.45-μm pore diameter). The dissolved protein was applied to a G-75 Sephadex (2.5 × 100 cm) column equilibrated with the same buffer. The proteins were eluted at a flow rate of 1 mL/min. Fractions of 2.5 mL were collected. GlTIM eluted after 140 mL had passed through the column. The fractions with TIM activity were pooled and concentrated in Amicon filters (YM 10) to a volume of 10 mL. The protein was dialyzed against 0.6 L of a buffer containing 10 mM Tris, 1 mM EDTA, pH 8.7. The enzyme was then applied to a Q-Sepharose FF (1.5 × 12 cm) column equilibrated and washed with the same buffer. GlTIM was eluted with a gradient of 30–100 mM NaCl. Fractions with activity were pooled and concentrated.

To increase the purity of the enzyme, GlTIM was applied to a SW300 (7.5 × 300 mm) column equilibrated with a buffer containing 50 mM triethanolamine hydrochloride, 10 mM EDTA, 150 mM NaCl, 30% glycerol, pH 7.5. Fractions with activity were pooled, concentrated, and stored at 4°C as a 50% glycerol solution in the same buffer. For the studies, the enzyme was dialyzed against a buffer containing 100 mM triethanolamine hydrochloride, 10 mM EDTA, pH 7.4. Densitometric analysis in sodium dodecyl sulfate-polyacrylamide gel electrophoresis (SDS-PAGE) under reducing conditions showed that GlTIM was >95% pure. This protocol was followed several times, and the enzyme yield ranged between 18 and 23 mg/L of culture. Table I summarizes the purification of GlTIM.

**TABLE I. Purification of Recombinant Triosephosphate Isomerase From *G. lamblia*[†]**

| Step | Total protein (mg) | Total activity (μmol GAP $min^{-1}$)[a] | Specific activity (μmol $min^{-1}$ $mg^{-1}$) |
|---|---|---|---|
| Homogenate (sonicated) | 336 | 559,440 | 1794 |
| G-75 column | 60 | 457,523 | 3305 |
| Q-Sepharose column | 20 | 76,000 | 3800 |

[†]The enzyme was purified as described in Materials and Methods, starting from 1-L culture.
[a]GAP, glyceraldehyde 3-phosphate.

*T. brucei* and *T. cruzi* recombinant TIMs were purified as previously described.[24,25] Protein concentration of pure TIM was determined spectrometrically at 280 nm. The molar extinction coefficients at 280 nm of TcTIM and TbTIM were 36440 and 34950, respectively.[25] The molar

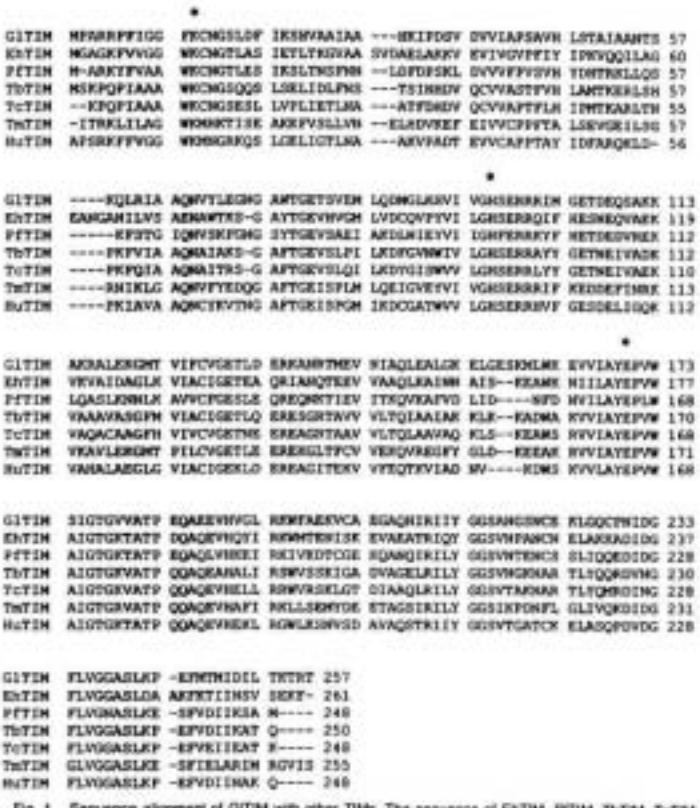

Fig. 1. Sequence alignment of GlTIM with other TIMs. The sequence of EhTIM, PfTIM, TbTIM, TcTIM, TmTIM, and HuTIM are shown. The active site residues are marked (*).

extinction coefficient of GlTIM was 26600, calculated according to Pace et al.[56]

To ascertain the best conditions for storage of GlTIM, the purified enzyme was incubated in buffers with different pH, maintaining a constant ionic strength. After this, aliquots were taken and diluted in a buffer containing 100 mM triethanolamine, 10 mM EDTA at pH 7.4. The activities of all samples were measured at this pH. The activity as a function of pH showed a bell-shaped curve, after it was incubated for 2 h, with a maximum activity between pH 6.5–9.0. The activity dropped significantly outside of this pH range. At pH 7.4, the activity of the enzyme was unaffected for at least 2 weeks.

### Activity Assays

Enzyme activity in the direction of GAP to DHAP was measured at 25°C by following the decay in absorbance at 340 nm of 1 mL reaction mixture at pH 7.4 that contained 100 mM triethanolamine, 10 mM EDTA, 0.2 mM NADH, 0.9 U α-glycerol-3-phosphate dehydrogenase, 1 mM GAP (except when catalytic constants were determined), and 10 ng TIM per mL. The kinetic constants were calculated from initial velocities ($v_i$) obtained at different substrate concentrations.

For the determination of Km, $k_{cat}$, and $K_i$ values for 2-phosphoglycolate (PG), the concentration of GAP ranged between 0.5 and 4 mM. The determination of catalytic constants in the direction of DHAP to GAP were determined at 25°C in 100 mM triethanolamine, 10 mM EDTA, 1 mM NAD, 4 mM arsenate, 120 μM dithiothreitol, 1 U glyceraldehyde 3-phosphate dehydrogenase per mL, 100 ng GlTIM per mL, and 0.3–10 mM DHAP.

### Polyclonal Anti-GlTIM Antibodies

Chickens (16-week-old Delkab-Warren) were immunized subcutaneously with 240 μg of highly purified GlTIM dissolved in complete Freund's adjuvant. The immunization dose was repeated two times at intervals of 1

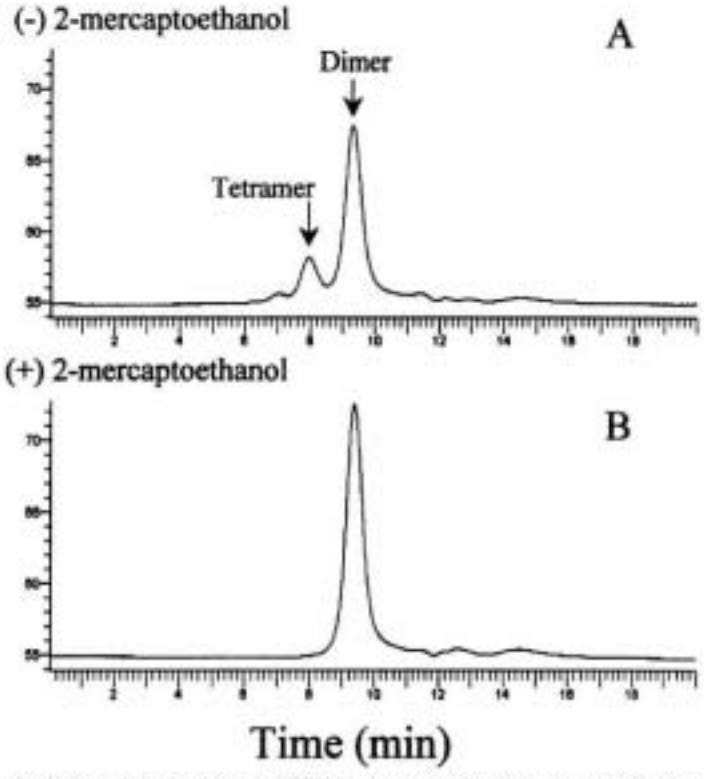


Fig. 2. Size exclusion chromatography of GITIM. The chromatographic analysis under nonreducing (A) and reducing (B) conditions were performed by using a SW300 column equilibrated with buffer containing 50 mM triethanolamine, 10 mM EDTA, 150 mM NaCl, 30% glycerol, pH 7.5. The proteins (25 μg) were eluted at a rate flow of 1 mL/min. For calibration, the following molecular weight markers were used: thyroglobulin, bovine γ-globulin, chicken ovalbumin, equine myoglobin, and vitamin $B_{12}$.

week. After the final boost, eggs were collected daily and processed individually. Chicken polyclonal antibodies (IgY) were purified from the egg yolk by using the method described by Polson et al.[27] The IgY proteins were dialyzed extensively against PBS buffer and applied to a size exclusion column equilibrated with the same buffer. The fractions enriched with IgY were pooled and concentrated. Western blot analysis was used to evaluate antibody specificity.

### Light and Electron Microscopy

For light microscopy, cells were grown over glass coverslips into six-well cell culture clusters (Costar). For electron microscopy, pellets of *G. lamblia* trophozoites with $\sim 10^6$ cells were obtained by centrifugation and embedded in acrylic resin Lowicryl K4M. Samples were fixed by using freshly prepared 4% paraformaldehyde in PBS.

### Immunocytochemistry

Coverslips with a monolayer of trophozoites were incubated in 0.5% Triton X-100 for 5 min at 4°C to permeate cells. Samples were rinsed with PBS and incubated on TBS buffer (20 mM Tris, pH 7.6, 150 mM NaCl, 20 mM $NaN_3$, 1% Tween 20, 5% BSA, 5% normal goat serum) for 1 h. Samples were incubated with anti-GITIM IgY diluted 1:4000 in PBS at 4°C overnight, rinsed with PBS, and incubated with rabbit anti-chicken IgG at 1:500 in PBS for 2 h at room temperature. Anti-rabbit IgG coupled to fluorescein isothiocyanate diluted 1:500 in PBS was used. Nuclei were stained by using DAPI (4′,6-diamidino-2-phenylindole) for specific DNA localization. Mounted samples were photographed with a fluorescence microscope (Axiovert 200; Carl Zeiss).

Ultrathin sections (~70 nm wide) were placed on nickel grids. Grids were floated on TBS buffer for 1 h and

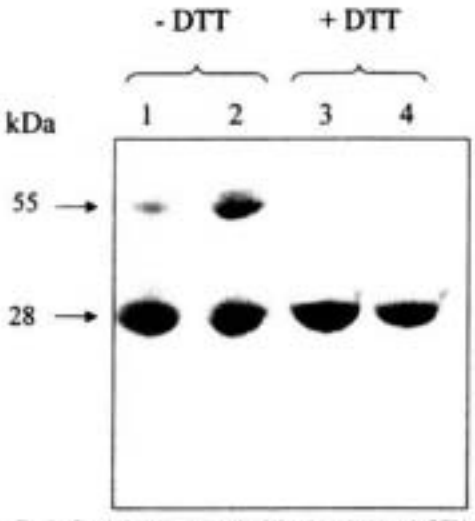


Fig. 3. Denaturing electrophoresis of dimeric and tetrameric GITIM. The samples that corresponded to tetrameric and dimeric GITIM were obtained from the chromatography fractions shown in Figure 2(A). Four micrograms of dimer (lanes 1 and 3) or 4 μg of tetramer (lanes 2 and 4, respectively) were analyzed by SDS-PAGE (12% acrylamide) according to Shägger and von Jagow,[27] under nonreducing (lanes 1 and 2) or reducing conditions (lanes 3 and 4).

incubated at 4°C overnight with a 1:4000 solution of anti-GITIM antibody. Grids were rinsed with PBS and incubated for 1.5 h with a secondary antibody against IgY (Jackson Immunoresearch) at 1:200 in PBS. Anti-rabbit IgG coupled to 10-nm colloidal gold particles (ICN) diluted 1:100 was added and incubated for 2 h. Samples were stained with 0.5% uranyl acetate and lead citrate for 1 min each. Photographs were taken in a transmission electron microscope (EM109; Carl Zeiss).

## RESULTS

### Sequence Analysis

In consonance with the data of Mowatt et al.,[12] we found that the gene of GITIM is formed by 774 pb with a predicted sequence of 257 amino acid residues and a molecular mass of 27,903 Da. Figure 1 shows the sequence alignment of TIMs from *G. lamblia* (GITIM), *Entamoeba histolytica* (EhTIM), *Plasmodium faleiparum* (PfTIM), *T. brucei* (TbTIM), *T. cruzi* (TcTIM), *T. maritima* (TmTIM), and human (HuTIM). The identity of GITIM with the enzymes from these organisms is 42, 41, 44, 46, 42, and 45%, respectively. From the amino acid sequence of GITIM, a pI of 7.05 was calculated. This is around 1 unit higher than the pI of TIM from *E. coli* (5.89). This allowed the separation of the two enzymes by ion exchange chromatography (see Materials and Methods). GITIM has five cysteines per monomer; human TIM has the same number of cysteines, but in different positions. The other enzymes have a lower number of cysteines. It is noted that except for TmTIM and HuTIM, the rest of enzymes have a cysteine in their interface (Cys 14 in GITIM). This region of the interface formed by the side-chain of Cys14 and its surrounding loop 3 of the other subunit has been described as a potential target for drug design.[28,29]

### Hydrodynamic Parameters and SDS-PAGE of GITIM

To explore the oligomerization state of GITIM, the enzyme was incubated overnight with or without the thiol-reducing agent 2-mercaptoethanol and then applied to an analytical SEC column (Fig. 2). The chromatographic profile of the enzyme incubated without 2-mercaptoethanol showed a minor peak with the Stokes radius of a protein with a molecular mass of 108 kDa and a major peak of 55 kDa. The enzyme that had been exposed to 2-mercaptoethanol showed only the 55-kDa protein. The peak that corresponded to the 55 kDa was larger for the enzyme treated with 2-mercaptoethanol. The same data were obtained when GITIM was incubated with dithiothreitol (data not shown).

To further examine the nature of the 55- and 108-kDa proteins, their electrophoretic profile in denaturing gel was determined in the *absence* of reducing agents (Fig. 3). In SDS-PAGE, the protein that had a mass of 55 kDa in size exclusion chromatography exhibited a main band of about 28 kDa and a minor band of about 55 kDa (Fig. 3, lane 1), which is probably a contamination with the 108-kDa protein. The 108-kDa protein showed two bands of Mw of about 55 kDa and 28 kDa. Under reducing conditions (dithiothreitol added), the high and low molecular weight proteins exhibited a single band of 28 kDa (Fig. 3, lanes 3 and 4). Both the 108- and 55-kDa proteins exhibited catalytic activity (see below).

Taken together, the results in Figures 2 and 3 indicate that recombinant GITIM may exist as a tetramer and a dimer of identical subunits. Moreover, the loss of the 108-kDa peak and the concomitant appearance of the 55-kDa protein under reducing conditions illustrate that in the tetramer, two GITIM dimers are joined by a disulfide bridge or bridges.

### Kinetics

The kinetics of GITIM were determined at different enzyme concentrations (0.1 or 0.2 nM). The traces of activity versus time were linear until NADH became limiting. Thus, the enzyme did not dissociate into monomers during the assay. As expected, the kinetic constants were independent of GITIM concentration. Lineweaver–Burk plots of the activity at different glyceraldehyde 3-phosphate concentrations (0.5–4 mM) were linear. The Km and $k_{cat}$ values of dimeric GITIM were similar to those reported for TIM from other species (Table II). The Km value of tetrameric enzyme was also in the range observed in other TIMs; however, its $k_{cat}$ was about half of that of the dimer (Table II). Using dihydroxyacetone as substrate (0.3–10 mM), the kinetic constants of the GITIM dimer were also similar to those reported for other TIMs. Be-

**TABLE II. Kinetic Constants of Recombinant GlTIM Compared With TIM From *T. brucei* (TbTIM) and Yeast (YtTIM)†**

| TIM | Km (GAP) mM | *kcat* (GAP) $min^{-1}$ | Km (DHAP) mM | *kcat* (DHAP) $min^{-1}$ | *Ki* (PG) mM |
|---|---|---|---|---|---|
| GlTIM dimer | 0.53 ± 0.03 | $(2.9 \pm 0.2) \times 10^5$ | 2.2 ± 0.2 | $(1.6 \pm 0.04) \times 10^4$ | 0.043 ± 0.005 |
| GlTIM tetramer | 0.87 ± 0.07 | $(1.47 \pm 0.04) \times 10^5$ | n.d. | n.d. | n.d. |
| TbTIM[a] | 0.35 | $2.6 \times 10^5$ | 1.9 | $2.7 \times 10^4$ | 0.024 |
| YtTIM[b] | 1.27 | $1 \times 10^6$ | 1.23 | $4.9 \times 10^4$ | 0.03 |

†Activities were determined with glyceraldehyde 3-phosphate (GAP) in the range of 0.5–4 mM; concentration ranged between 0.3 and 10 mM for dihydroxyacetone phosphate (DHAP); PG is 2-phosphoglycolate. The conditions of the reaction are described in Materials and Methods. The values are the averages (±SE) of three independent experiments.
[a]Data from Hernández-Alcántara et al.[29]
[b]Data from Lambeir et al.[31]

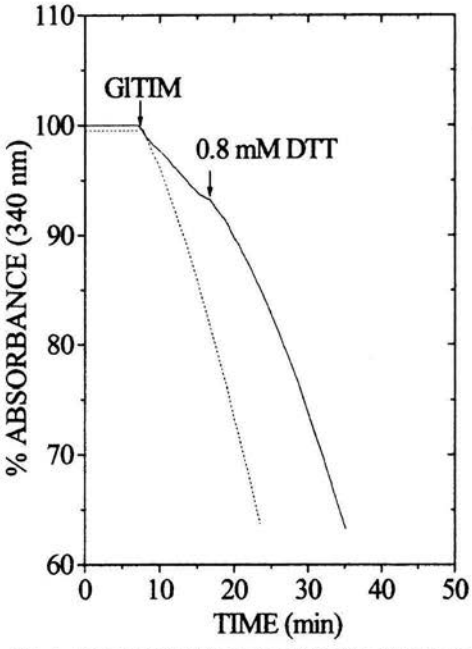


Fig. 4. Effect of dithiothreitol on the activity of the tetramer. The activities of the dimer (dashed line) and the tetramer (solid line) were followed spectrophotometrically at 340 nm. The arrows indicate the addition of 2.5 ng of dimer or tetramer to 1 mL reaction mixture (see Materials and Methods). The addition of 0.8 mM dithiothreitol is also indicated.

cause of its sensitivity to reducing agents (see Figs. 2 and 3), the kinetics of the tetramer in the direction of dihydroxyacetone to glyceraldehyde 3-phosphate could not be determined. Because the $k_{cat}$ of the tetramer was lower than that of the dimer, we explored if the conversion of tetramer to dimers brought about an increase in activity. Indeed, we observed that the addition of dithiothreitol to tetrameric GlTIM undergoing active catalysis induced an increase in the rate at which the enzyme converts GAP to DHAP (Fig. 4). Under the conditions of the experiment, a rate equal to that of the dimer was attained in ~15 min after the addition of dithiothreitol.

The inhibition constant ($K_i$) of the transition-state analog 2-phosphoglycolate was determined for the dimeric enzyme (Table II). The $K_i$ value was close to that reported for trypanosomal and yeast TIMs.[30]

### Stability of GlTIM at Different Concentrations

The interface of dimeric TIM is formed by noncovalent interactions between TIM monomers; the association constant of the two subunits is in the order of $10^{-10}$ to $10^{-16}$ M.[31–35] Because in its monomeric state the enzyme is catalytically inactive,[30,36,37] the loss of the dimeric state can be followed by the activity of the enzyme after it has been incubated at different concentrations. The apparent dissociation constant ($K_D^{app}$) between the two monomers can be calculated from the data. Therefore, to gain insight into the dissociation constants between the monomers of GlTIM, the tetramer and the dimer were incubated at concentrations that ranged from 0.0025 to 500 μg/mL. After 2 h of incubation, the specific activity of the two enzymes was determined.

The curves of percent of specific activity versus enzyme concentration of the dimer and tetramer of GlTIM were sigmoid (Fig. 5), as observed with other TIMs.[38] At low protein concentrations, the specific activity of tetramer and dimer of GlTIM was low; however, as the concentration of protein was raised, the specific activity of the two enzymes increased until it reached a constant level. From the data, the $K_D^{app}$ was calculated. As shown in Figure 5, the apparent dissociation constant between the monomers of dimeric ($50.6 \pm 12 \times 10^{-9}$ M) and tetrameric ($9.8 \pm 0.6 \times 10^{-9}$ M) GlTIM was slightly lower than that of TcTIM ($44 \pm 2.3 \times 10^{-9}$ M) and TbTIM ($43.8 \pm 4 \times 10^{-9}$ M). It is also noteworthy that the $K_D^{app}$ of the dimer and tetramer of GlTIM was in the same range. These findings suggest that the tetramer results from the covalent attachment of two dimers that conserve similar association constants between their constituent monomers.

A point that is worth noting is that enzyme concentrations of the order of 0.2 nM were used for measurements of activity. According to the data of Figure 5, it could be expected that at concentrations of 0.2 nM, there would be dissociation of the subunits of GlTIM. However, it is recalled that the occupancy of the catalytic site increases the stability of TIM.[25,39,40] Moreover, in the conditions used for Figure 5, loss of activity is a rather slow process.

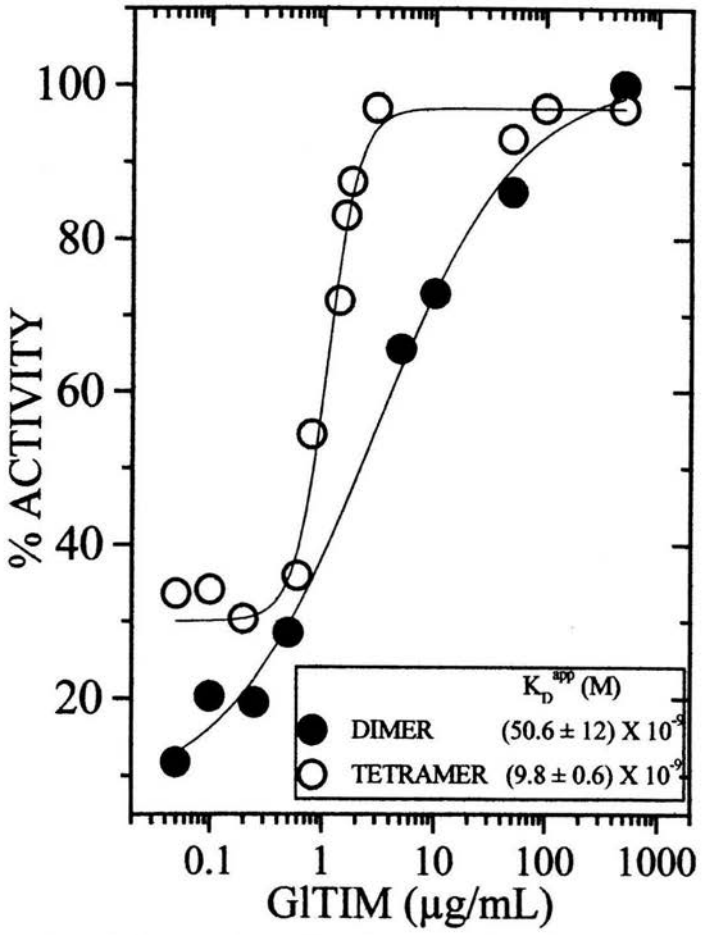


Fig. 5. Stability of the dimer and tetramer of GlTIM at different concentrations. The dimer and tetramer were incubated at concentrations that range from 0.0025 to 500 μg/mL at 40°C in a buffer containing 100 mM triethanolamine, 10 mM EDTA, pH 7.4. After 2-h samples were incubated for 1 min at 25°C, subsequently the residual activity was determined with 10 ng of protein/mL reaction mixture. The percent of specific activity versus enzyme concentration is shown; 100% of activity was 1700 and 714 μmol $min^{-1}$ $mg^{-1}$ for the dimer and tetramer, respectively. The apparent $K_D$ (±SE) of three independent experiments were calculated and fitted with nonlinear regression plots.

Thus, in the times in which activity was measured, no dissociation to monomers took place. Indeed, we always observed that the activity traces were linear with time.

### Stability to Temperature

The thermostabilities of the dimer and the tetramer of GlTIM were determined from measurements of the decay of activity at different temperatures. The data were compared with those of TcTIM and TbTIM. In all cases, inactivation followed a simple exponential decay. Thus, the data were expressed as $k_{obs}$ (Table III). At 45 and 55°C, the GlTIM dimer exhibited the highest decay rate. At 60°C, however, the rate of inactivation was similar in the four enzymes. It is noted that the loss of activity in the tetramer was not markedly different from that of the other enzymes tested, albeit at 45 and 55°C, it was slightly more stable than the dimer.

**TABLE III. First-Order Rate Constants for Inactivation as a Function of Temperature for GlTIM, TcTIM, and TbTIM[†]**

| | $k_{obs}$ ($h^{-1}$) | | |
|---|---|---|---|
| TIM | 45°C | 55°C | 60°C |
| GlTIM dimer | 1.9 ± 0.1 | 65 ± 3 | 173 ± 9 |
| GlTIM tetramer | 0 | 43 ± 5.4 | 169 ± 7.5 |
| TcTIM | $(4 \pm 0.37) \times 10^{-2}$ | 36 ± 4.3 | 198 ± 17 |
| TbTIM | $(9 \pm 0.72) \times 10^{-2}$ | 23.04 ± 1.44 | 120 ± 2.4 |

[†]The enzymes were incubated at 100 μg/mL in 100 mM triethanolamine, 10 mM EDTA buffer (pH 7.4) at the indicated temperatures. At different times of incubation, aliquots were withdrawn and activities measured at 25°C. The $k_{obs}$ (±SE) were calculated from nonlinear regression plots.

### In Situ Localization of GlTIM

Fluorescence immunolocalization of cellular GlTIM showed that the enzyme was quite abundant in all the cytoplasm of *G. lamblia* trophozoites [Fig. 6(A), anti-GlTIM panel]. Its distribution was uniform, albeit the nuclei were not labeled [Fig. 6(A), DAPI panel]. Electron microscopy corroborated the homogeneous cellular distribution of GlTIM [Fig. 6(B)]; that is, the enzyme is not contained in membranous vesicles (as in the glycosomes of trypanosomes).[41]

## DISCUSSION

The kinetics, the association constant between monomers, and the thermostability of GlTIM are similar to those of other TIMs. Nonetheless, in size exclusion chromatography, two catalytically active proteins with molecular masses of 108 and 55 kDa were clearly evident. The same results were obtained when the catalytically active proteins were analyzed in nonreducing native gel electrophoresis. It is also noteworthy that only the 28-kDa protein was observed in SDS-PAGE under reducing conditions, whereas in the absence of reducing agents, two proteins with molecular masses of 55 and 28 kDa were detected. Taken together, these findings indicate that TIM from *G. lamblia* can exist as a tetramer or a dimer of identical subunits. Moreover, because reducing agents induce the transformation of tetramers to dimers, it may be concluded that two GlTIM dimers are covalently linked by disulfide bonds in the tetramer. In this regard, it is noted that in the tetramer, the linkage of two dimers must be through an -S-S- bridge between only one of the monomers of each dimer; otherwise, the tetrameric form in SDS-PAGE under nonreducing conditions would have exhibited only the 55-kDa protein; instead, the gel showed bands of 55 and 28 kDa.

GlTIM has cysteines at positions 14, 127, 202, 222, and 228. PfTIM has cysteines at positions 13, 126, 196, and 217. The cysteines of PfTIM and GlTIM have different positions in the primary sequence. This is because GlTIM has an insertion of seven residues. However, the positions of the cysteines between both organisms are equivalent (Fig. 1). Therefore, the crystal structure of the PfTIM[42] was used to model the accessible solvent area (ASA) of the five cysteines of GlTIM. The predicted ASA of the five lateral chains of the cysteines from GlTIM[43] showed that Cys 202, located in helix 6, could be the residue most exposed to solvent (47.1 Å$^2$). Alternatively, GlTIM possesses a Cys 228 residue, but the residue that PfTIM contains at this equivalent position is Gln 223. Consequently, Cys 228 of GlTIM would be located on loop 8 with also a highly predicted ASA (26.7 Å$^2$). Therefore, it is probable that the cysteines involved in the disulfide of the tetramer were either Cys 202 or Cys 228 from each dimer.

As noted, TIM from *T. maritima* is a tetramer fused with phosphoglycerate kinase.[44] The crystal structure of the tetrameric TIM after it was separated from glycerate kinase by molecular engineering has been reported.[21] In this tetramer, the two dimers are linked through contacts between hydrophobic and polar residues; however, the predominant linkages in the tetramer are the two disulfide bonds that are established between cysteines 142 of each monomer. In regard to the structural features of TIM from *T. maritima*, it has been proposed that through tetramerization, the enzyme acquires a higher thermostability.[44] Here, we found that the dimer and tetramer of GlTIM do not exhibit important differences in thermostability nor in their association constant between monomers. Therefore, it is possible that in the mesophile *G. lamblia*, the occurrence of tetrameric and dimeric forms serves a different purpose.

In the latter respect, the comparison of the kinetics of the GlTIM dimer and tetramer may be illustrative. The data show that although the two enzymes have the same Km for glyceraldehyde 3-phosphate, the $k_{cat}$ of the tetramer is about half of that of the dimer. This suggests that the tetramer is an enzyme with only two catalytically competent sites. In this connection, it is relevant to point out that TIM dimers, in which one of its two catalytic sites has been poisoned with a covalently linked inhibitor, express 50% of its maximal activity without important changes in Km,[45,46] indicating that the catalytic sites of two monomers work independently. However, Biemann and Koshland[47] reported that a protein with two potential binding sites exhibited Michaelis–Menten behavior with a Hill coefficient of 1 and that, nonetheless, the protein expressed what they called half of the site reactivity. That is, the occupancy of one binding site suppressed the function of the other site. With the present data, it is not possible to distinguish between the two alternatives. However, it is noted that the kinetics of the dimer and tetramer exhibited classical Michaelis–Menten behavior with Hill coefficients of 1.1 and 1.02, respectively.

In sum, our data on TIM from *G. lamblia* show that it has characteristics that set it apart from all the other TIMs so far reported. Indeed, to our knowledge, GlTIM is the first example of a TIM from a mesophile that may acquire a tetrameric structure. Likewise, GlTIM is also the only known eukaryotic TIM that can acquire a tetrameric structure. Along this line, it may not be a coincidence that *G. lamblia* is one of the earliest branches of eukaryotes. In addition, from the point of view of catalytic mechanisms, GlTIM also seems rather unique, because the kinetics of

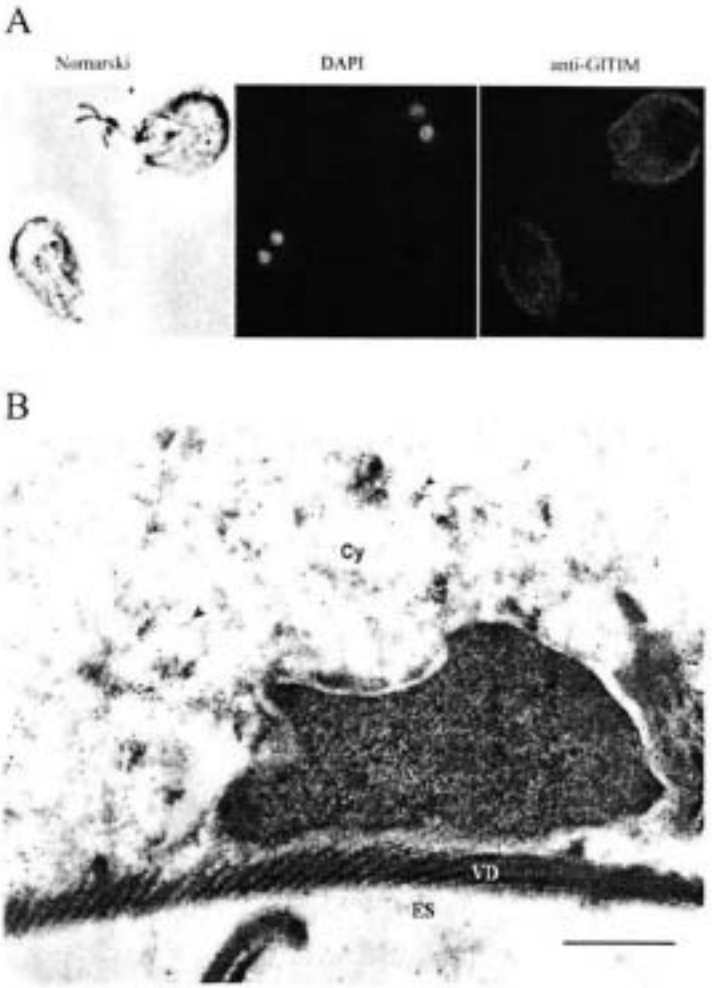


Fig. 8. (A) Immunofluorescence of cellular GITIM and (B) its distribution at the electron-microscopical level. Colloidal gold particles (arrow heads) show the localization of GITIM. ES, extracellular space; VD, ventral disc; Cy, cytoplasm; N, nucleus. Bar 0.5 μm.

the enzyme showed that in the tetramer only two of its four catalytic sites are catalytically competent.

The aforementioned considerations raise the question of whether the characteristics of GITIM, particularly in its ability to tetramerize with a concomitant decrease in catalytic efficiency, are of physiological significance. Implicit in this question is the possibility that tetramerization of GITIM is an "artifact" of laboratory manipulations during its purification or storage. Indeed, when we carry out the purification procedure with solutions supplemented with DTT, we only observed GITIM dimers. This is what would be expected if the tetrameric structure were maintained by disulfide bounds. Nonetheless, regardless of whether tetramerization is of physiological significance, the fact remains that dimers of GITIM are prone to tetramerization. In fact, we have observed that in a few hours at room temperatures, ~5% of the dimers are transformed into tetramers. Conversely, under reducing conditions, tetramers are converted into dimers with a corresponding gain in catalytic activity. Thus, the possibil-

ity that tetramerization is relevant to the life of the parasite should be considered. The life cycle of *G. lamblia* involves transformation of cysts into trophozoites; therefore, it could be that the transition of GITIM tetramers to dimers, or vice versa, is guided by the intracellular conditions in a given physiological state. The tetramer could be a "storage conformation," which participates in a transition from a state with a low metabolism toward a higher metabolic state. Thus, it seems clear that the reversible reaction between GITIM dimers and tetramers deserves further studies.

Before closing, we call attention to two points that arose from the data of this work. The first is that, although the bulk of eukaryotic genome appears to share common ancestry with archaeobacteria,[46,49] the phylogenetic analysis of the TIM gene from several species (including *G. lamblia*) supports the notion that eukaryotic TIM has an alpha-proteobacterial origin.[50] Therefore, it would be interesting to determine if the different oligomerization states of GITIM are a consequence of parasitic adaptations or whether they are an archaebacterial relic. Finally, the data on the intracellular localization of GITIM show that it is an enzyme that is evenly distributed throughout the cytoplasm and separated from the extracellular milieu only by the cytoplasmic membrane. Therefore, the penetration of drugs that target on GITIM would not be hindered by internal permeability barriers.

## ACKNOWLEDGMENTS

D.M.-O. is the recipient of a fellowship from CONACyT. The authors are indebted to Dr. M. Tuena de Gómez-Puyou and Dr. A. Gómez-Puyou for their advice on the improvement of the manuscript. We also thank Dr. E. Chávez Cosio for invaluable help on IgY development, Dr. Antonio Lazcano-Araujo for his comments of the manuscript, and Janet Flores for providing us with HPLC resources. The technical assistance of Carmen Ortiz, Sara Navarrete, and Amparo Tapia is acknowledged.

## REFERENCES

1. Edlin TD, Chakraborty PR. Unusual ribosomal RNA of the intestinal parasite *Giardia lamblia*. Nucleic Acids Res 1987;15: 7889–7901.
2. Segin ML, Gunderson JH, Elwood HJ, Alonso RA, Peattie DA. Phylogenetic meaning of the kingdom concept: an unusual ribosomal RNA from *Giardia lamblia*. Science 1989;6:75–77.
3. Nasvisi EM, Glover VC, Fechheimer M. Fibrillarin, a conserved pre-ribosomal RNA processing protein of *Giardia*. J Euk Microbiol 1996;45:105–111.
4. Hilario E, Gogarten JP. The prokaryote-to-eukaryote transition reflected in the evolution of the V/F/A-ATPase catalytic and proteolipid subunits. J Mol Evol 1998;46:703–715.
5. Adam RD. The *Giardia lamblia* genome. Int J Parasitol 2000;30: 475–484.
6. Boreham PFL. Giardiasis and its control. Pharm J 1991;234:271–274.
7. Townson SM, Boreham PFL, Upcroft P, Upcroft JA. Resistance to the nitroheterocyclic drugs. Acta Trop 1994;56:173–194.
8. Upcroft J , Upcroft P. My favorite cell: *Giardia*. BioEssays 1998;20:256–263.
9. Upcroft J, Upcroft P. Drug resistance and *Giardia*. Parasitol Today 1993;9:187–190.
10. Müller M. Energy metabolism of ancestral eukaryotes: a hypothesis based on the biochemistry of the amitochondriate parasitic protists. Biosystems 1992;28:33–40
11. Schofield PJ, Edwards MR, Kranz P. Glucose metabolism in *Giardia intestinalis*. Mol Biochem Parasitol 1991;45:39–48.
12. Mowatt MR, Weinbach EC, Howard TC, Nash TE. Complementation of an *Escherichia coli* glycolysis mutant by *Giardia lamblia* triosephosphate isomerase. Exp Parasitol 1994;78:85–92.
13. Albery J, Knowles JR. Evolution of enzyme function and the development of catalytic efficiency. Biochemistry 1976;64:5631–5640.
14. Albert T, Banner DW, Bloomer AC, Petsko GA, Phillips C, Rivers P S, Wilson IA. On the three-dimensional structure and catalytic mechanism of triosephosphate isomerase. Phil Trans Roy Soc B 1981;293:159–171.
15. Nickbarg EB, Knowles JR. Triosephosphate isomerase; energetics of the reaction catalyzed by the yeast enzyme expressed in *Escherichia coli*. Biochemistry 1988;27:5939–5947.
16. Knowles JR. Enzyme catalysis; not different, just better. Nature 1991;350:121–124.
17. Bell GS, Russell RJ, Kohlhoff HM, Hensel R, Danson MJ, Hough DW, Taylor GL. Preliminary crystallographic studies of triosephosphate isomerase (TIM) from the hyperthermophilic Archaeon *Pyrococcus woesei*. Acta Crystallogr Sect D Biol Crystallogr 1998; 54:1419–1421.
18. Walden H, Bell GS, Russell RJM, Siebers B, Hensel R, Taylor GL. Tiny TIM: a small, tetrameric, hyperthermostable triosephosphate isomerase. J Mol Biol 2001;306:745–757.
19. Kohlhoff M, Dahm A, Hensel R. Tetrameric triosephosphate isomerase from hyperthermophilic archaea. FEBS Lett 1996;383: 245–250.
20. Yu JS, Noll KM. The hyperthermophilic bacterium *Thermotoga neapolitana* possesses two isozymes of the 3-phosphoglycerate kinase/triosephosphate isomerase fusion protein. FEMS Microbiol Lett 1995;131:307–312.
21. Maes D, Zeelen JP, Thanki N, Beaucamp N, Alvarez M, Thi MHD, Backmann J, Martial JA, Wyns L, Jaenicke R, Wierenga R. The crystal structure of triosephosphate isomerase (TIM) from *Thermotoga maritima*: a comparative thermostability structural analysis of ten different TIM structures. Proteins 1999;37:441–453.
22. Mowatt MR, Aggarwal A, Nash TE. Carboxy-terminal sequence conservation among variant-specific surface proteins of *Giardia lamblia*. Mol Biochem Parasitol 1991;4:215–228.
23. López-Velázquez G, Segura-Valdez MA, Alcántara-Ortigoza MA, Jiménez-García LF. Localization of intranuclear RNA by electron microscopy in situ hybridization using a genomic DNA probe. Arch Med Res 1998;29:185–190.
24. Borchert TV, Pratt K, Zeelen JP, Callens M, Noble ME, Opperdoes FR, Michels PA, Wierenga RK. Overexpression of trypanosomal triosephosphate isomerase in *Escherichia coli* and characterization of a dimer-interface mutant. Eur J Biochem 1993;213:684–691.
25. Ostoa-Saloma P, Garza-Ramos G, Ramírez J, Becker I, Berzunza M, Landa A, Gómez-Puyou A, Gómez-Puyou MT, Pérez-Montfort R. Cloning, expression, purification and characterization of triosephosphate isomerase from *Trypanosoma cruzi*. Eur J Biochem 1997;244:700–705.
26. Pace NC, Vajdos F, Fee L, Grimsley G, Gray V. How to measure and predict the molar absorption coefficient of a protein. Protein Sci 1995;4:2411–2423.
27. Palese A, von Wechmar B, Van Regenmortal MHV. Isolation of viral IgY antibodies from yolks of immunized hens. Immunol Comm 1980;9:475–493.
28. Garza-Ramos G, Pérez-Montfort R, Rojo Domínguez A, Tuena de Gómez-Puyou, M, Gómez-Puyou A. Species-specific inhibition of homologous enzymes by modification of non-conserved amino acids residues. The cysteine residues of triosephosphate isomerase. Eur J Biochem 1996;241:114–120.
29. Hernández-Alcántara G, Garza-Ramos G, Mendoza-Hernández G, Gómez-Puyou A, Pérez-Montfort R. Catalysis and stability of triosephosphate isomerase from *Trypanosoma brucei* with different residues at position 14 of the dimer interface. Characterization of a catalytically competent monomeric enzyme. Biochemistry 2002;41:4230–4238.
30. Garza-Ramos G, Tuena de Gómez-Puyou M, Gómez-Puyou A, Gracy RW. Dimerization and reactivation of triosephosphate isomerase in reverse micelles. Eur J Biochem 1992;206:389–395.
31. Lambeir AM, Opperdoes BF, Wierenga RK. Kinetic properties of triose-phosphate isomerase from *Trypanosoma brucei*. Eur J Biochem 1987;168:69–74.

32. Mainfroid V, Terpstra P, Beauregard M, Frère JM, Mande SC, Hol WG, Martial JA, Goraj K. Three hTIM mutants that provide new insights on why TIM is a dimer. J Mol Biol 1996;257:441–456.
33. Landa A, Rojo-Domínguez A, Jiménez L, Fernández-Velasco A. Sequencing, expression and properties of triosephosphate isomerase from *Entamoeba histolytica*. Eur J Biochem 1997;247:348–355.
34. Borchert TV, Pratt K, Zeelen JP, Callens M, Noble ME, Opperdoes FR, Michels PA, Wierenga RK. Overexpression of trypanosomal triosephosphate isomerase in *Escherichia coli* and characterization of a dimer-interface mutant. Eur J Biochem 1993;211:703–710.
35. Borchert TV, Abagyan R, Jaenicke R, Wierenga RK. Design, creation, and characterization of a stable, monomeric triosephosphate isomerase. Proc Natl Acad Sci USA 1994;91:1515–1518.
36. Waley SG. Refolding of triosephosphate isomerase. Biochem J 1973;135:165–172.
37. Zaberi S, Rudolph F, Jaenicke R. Folding and association of triosephosphate isomerase from rabbit muscle. Z Naturforsch 1980;35:999–1004.
38. Reyes-Vivas H, Martínez-Martínez E, Mendoza-Hernández G, López-Velázquez G, Pérez-Montfort R, Tuena de Gómez-Puyou M, Gómez-Puyou A. Susceptibility to proteolysis of triosephosphate isomerase from two pathogenic parasites: characterization of an enzyme with an intact and a nicked monomer. Proteins 2002;48:580–590.
39. Long CW, Levitzki A, Koshland DE. The subunit structure and subunit interactions of cytidine triphosphate synthetase. J Biol Chem 1970;10:80–87.
40. Jiménez L, Fernández-Velasco DA, Willms K, Landa A. A comparative study of biochemical and immunological properties of triosephosphate isomerase from *Taenia solium* and *Sus scrofa*. J Parasitol 2003;89:209–214.
41. Opperdoes FR, Borst P. Localization of nine glycolytic enzymes in a microbody-like organelle in *Trypanosoma brucei*: the glycosome. FEBS Lett 1977;80:360–364.
42. Velanker SS, Ray SS, Gokhale RS, Suma S, Balaram H, Balaram P, Murthy MRN. Triosephosphate isomerase from *Plasmodium falciparum*: the crystal structure provides insights into antimalarial drug design. Structure 1997;5:751–761.
43. Gerstein M. A resolution-sensitive procedure for comparing protein surfaces and its application to the comparison of antigen-combining sites. Acta Crystallogr 1992;A48:271–276.
44. Beaucamp N, Hofmann A, Kellerer B, Jaenicke R. Dissection of the gene of the bifunctional PGK-TIM fusion protein from the hyperthermophilic bacterium *Thermotoga maritima*: design and characterization of the separate triosephosphate isomerase. Protein Sci 1997;6:2159–2165.
45. Schnackerz DD, Gracy RW. Probing the catalytic sites of triosephosphate isomerase by $^{31}$P-NMR with reversibly and irreversibly binding substrate analogues. Eur J Biochem 1991;199:231–238.
46. Sun A-Q, Yüksel Ü, Gracy RW. Interactions between the catalytic centers and subunit interface of triosephosphate isomerase probed by refolding, active site modification, and subunit exchange. J Biol Chem 1992;267:20168–20174.
47. Biemann HP, Koshland DE. Aspartate receptor of *Escherichia coli* and *Salmonella typhimurium* bind ligand with negative and half-of-the sites cooperativity. Biochemistry 1994;33:629–634.
48. Iwabe N, Kuma KI, Hasegawa M, Osawa S, Miyata T. Evolutionary relationship of archaebacteria, eubacteria, and eukaryotes inferred from phylogenetic trees of duplicated genes. Proc Natl Acad Sci USA 1989;86:9355–9359.
49. Brown JR, Doolittle WF. Root of the universal tree of life based on ancient aminoacyl-tRNA synthetase gene duplications. Proc Natl Acad Sci USA 1995;92:2441–2445.
50. Keeling PJ, Doolittle WF. Evidence that eukaryotic triosephosphate isomerase is of alpha-proteobacterial origin. Proc Natl Acad Sci USA 1997;94:1270–1275.
51. Shägger H, von Jagow G. Tricine-sodium dodecyl sulphate polyacrylamide gel electrophoresis for the separation of proteins in the range from 1 to 100 kDa. Anal Biochem 1987;166:368–379.

**Electron Microscopy Analysis of the Nucleolus of *Trypanosoma cruzi***

**Gabriel López-Velázquez[1,2], Roberto Hernández[3], Imelda López-Villaseñor[3], Horacio Reyes-Vivas[2], María de L. Segura-Valdez[3] and Luis F. Jiménez-García[1]**

[1] *Department of Cell Biology, Faculty of Sciences, UNAM, D.F.,04510, México*

[2] *Biochemistry and Genetics Laboratory, National Institute of Pediatrics, S.S., D.F., 04530, México*

[3] *Department of Molecular Biology and Biotechnology, Biomedical Research Institute, UNAM, D.F., 04510, México.*

Corresponding Author:

Luis F. Jiménez-García

Departamento de Biología Celular

Facultad de Ciencias, UNAM

México D.F. 04510, México

Telephone number: (52) 562-251-57;

FAX number: (52) 562-248-28

Email: lfjg@hp.fciencias.unam.mx.

**ABSTRACT**

The nucleolus is the main site for synthesis and processing of ribosomal RNA in eukaryotes. In mammals, plants, and yeast the nucleolus has been extensively characterized by electron microscopy, but in the majority of the unicellular eukaryotes no such studies have been performed. Here we used ultrastructural, cytochemical, and immunocytochemical techniques as well as 3D reconstruction to analyze the nucleolus of *Trypanosoma cruzi* which is an early divergent eukaryote of medical importance. In *T. cruzi* epimastigotes the nucleolus is a spherical intranuclear ribonucleoprotein organelle localized in a relative central position within the nucleus. Dense fibrillar and granular components but not fibrillar centers were observed. In addition, nuclear bodies resembling Cajal bodies were observed associated to the nucleolus in the surrounding nucleoplasm. Our results provide additional morphological data to better understand the synthesis and processing of the ribosomal RNA in kinetoplastids.

**Key Words.** Cajal bodies, nucleolus, nucleus, ribosomal RNA, *Trypanosoma cruzi*.

## Introduction

The mammalian cell nucleus is a highly compartmentalized and very dynamic organelle related to several steps of RNA metabolism (Spector, 1993, 2001; Lamond and Earnshaw, 1998; Misteli, 2001). The nucleolus is a ribonucleoprotein compartment where transcription and processing of pre-rRNA and ribosome assembly take place involving many molecules as rDNA, non processed, and mature forms of rRNA, proteins, and UsnRNA. These molecules are organized in ultrastructural compartments known as fibrillar centers (FCs), dense fibrillar (DFC), and granular component (GC) (see Spector, 1993; Busch and Smetana, 1970; Jordan and Cullis, 1982; Risueño and Medina, 1986; Shaw and Jordan, 1995; Thiry and Goessens, 1996; Scheer and Hock, 1999; Sewarzacher and Mosgoller, 2000; Huang, 2002). It is widely accepted that nucleolar transcription and early pre-rRNA processing take place in the fibrillar portion of the nucleolus while the late steps of processing and ribosome assembly occur mainly in the granular region. While this organization of nucleolar structure is well known in mammals and also but in lesser extent in plants and yeast, unicellular eukaryotes have not been studied in detail by electron microscopy, as for example members of the trypanosomatids where molecular biology studies are abundant.

*Trypanosoma cruzi*, the causative agent of Chagas' disease in humans, afflicts millions of people in America and is of a clear medical and economical importance (Herwalt, 1999). It is estimated that 16-18 million people may currently be infected and up to 100 million may be at risk of infection in the continent (WHO, 1997). On the other hand, trypanosomes are early divergent unicellular eukaryotes that show several atypical mechanisms of gene expression. Polycistronic transcription units and trans-splicing of messenger RNAs are interesting phenomena presents in these organisms (Agabian, 1990). Nevertheless, they also share several characteristics proper of more evolved eukaryotes. For example, molecules which participate on cis-splicing as U1, U2, U4, U5, U6 snRNAs, and SR proteins had been described (Ismaili et al., 1999; Djikeng et al., 2001). Ribosomal RNA (rRNA), the major transcription product of all living cells, has been extensively studied in trypanosomes, mainly at a molecular level. As in all trypanosomatids analyzed to date, cytosolic rRNA from *T. cruzi* is atypical in that the large subunit is composed of two large and five small independent rRNAs (Hernández et al., 1998). These molecules are encoded as different modules in a so-called main transcription unit. The transcription units are present in about 100 copies per nucleus, separated by sequences longer than 20kb, and are encoded in at least two chromosomes (Hernández et al., 1998; Castro et al., 1981; Wagner and So, 1990). There are several molecules involved in rRNA synthesis and maturation in trypanosomes, which are shared with higher eukaryotes. C/D box small nucleolar RNAs (snoRNAs) like U3 and other snoRNAs involved in rRNA methylation, fibrillarin, and RNA polymerase I have been previously described (Hartshorne and Agabian, 1993; Jess et al., 1989; Dunbar et al., 2000). Recently, it was shown that nucleolar transcription decreases from epimastigote to trypomastigote stages in *T. cruzi*, which also correlated to a gradual reduction in nucleolar size until this organelle disappears (Elias et al., 2001) . Because epimastigotes are very active in transcription, we have analyzed the nucleolar ultrastructure to identify nucleolar domains involved in rRNA formation. We found that there are not fibrillar centers in this parasite. In addition, nucleolar material is present in nuclear bodies. The ultrastructure analysis presented in this paper will complement molecular data on the nucleolus of *T. cruzi* and therefore will help in understanding the ribosome biogenesis in this parasite.

**Materials and methods**

*Parasites.* *T. cruzi* epimastigotes from clone CL Brener were grown at 28° C in liver infusion tryptose medium (LIT), supplemented with 10% fetal calf serum. Parasites were harvested at medial phase of logarithmic grow (ten to thirty-five million cells per ml) and washed with PBS.

*Transmission Electron Microscopy.* Pellets of *T. cruzi* with around $10^6$ cells were obtained by centrifugation, and processed for standard transmission electron microscopy (Vázquez-Nin and Echeverría, 2000) fixed using either 2.5% glutaraldehyde in PBS, post-fixed in 1% osmium tetroxide and embedded in epoxic resin. Semithin sections of about 250 nm width were stained with toluidine blue and observed with bright field microscopy. Thin sections were mounted on copper grids and contrasted with uranyl acetate and lead citrate.

*Serial sectioning.* Samples embedded in Epon were cut with an ultramicrotome Series of 80 sections of ≈70 nm width each were obtained and mounted onto Sjöstrand rings previously coated with a formvar film as described (Wettstein and Graver, 1973). Samples were then stained with uranyl acetate and lead citrate. The sections containing the whole nucleolus were photographed in a transmission electron microscopy at a fixed magnification (X25, 000).

*Image processing.* Images from serial sections were digitized and processed using a computing package (Imagenia 5000, Biocom) compatible with IBM PC. Three dimensional display and morphological measurements were carried out using specialized software based on boxels, as previously described (López-Velázquez et al., 1996).

*AgNOR staining.* Parasite pellets fixed in 2.5% glutaraldehyde were processed using the technique for nucleolar organizer (AgNOR) (Goodpasture and Bloom, 1975) with modifications for postembedding ultrastructural analysis (Spector et al., 1998). Samples were embedded in epoxy resin and cut as described above. Sections were placed onto copper grids and uranyl-lead stained.

*Ribonucleoproteins staining.* A set of samples fixed with 2.5% glutaraldehyde were not postfixed with osmium tetroxide, then embedded in epoxy resin and mounted in copper grids to perform the regressive method preferential for ribonucleopreoteins (Bernhard, 1969). Grids were treated with 0.5% uranyl acetate for 10 min, EDTA 0.2 M, pH 7.0 for 45 min, and lead citrate for 5 min.

*Immunocytochemistry.* Immunodetection was performed according to reported protocols (Roth, 1986) with modifications. Briefly, samples were fixed in 4% paraformaldehyde and embedded in Lowicryl resin. Sections were mounted onto nickel grids. Grids were floated on TBS buffer (20mM Tris, pH 7.6, 150 mM NaCl, 20 mM $NaN_3$, 1% Tween 20, 5% BSA, 5% NGS) for 1h, washed three times in PBS and incubated at 4°C over night with a mouse IgM anti-DNA antibody. After this, grids were washed in PBS and incubated for 90 min with a secondary antibody coupled to 12-15 nm colloidal gold particles.

## Results

To test the presence of nucleolar material in *T. cruzi* detected by light microscopy, we used bright field microscopy to analyze semithin sections of electron microscopy processed material after silver staining for nucleolar organizer. The results showed intense contrasted material in the nuclei of *T. cruzi* (Figure 1) but not in other cell compartments.

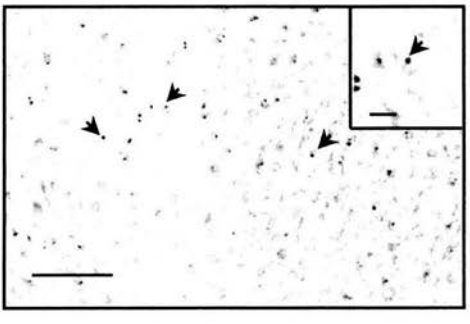

**Figure 1.** Silver staining for nucleolar organizer on acrylic-embedded semithin sections of *T. cruzi*. Arrows show a single spherical intranuclear body per cell intensely labeled. Inset shows a magnification of a single cell. Bar: 10 μm, inset bar: 2 μm.

Transmission electron microscopy of glutaraldehyde fixed parasites was performed to test for nucleolar components. One single rounded fibrogranular body per nucleus, in a central or somewhat polarized position into the nucleoplasm was observed (Fig. 2a). This body corresponds to the nucleolus and is surrounded by nuclear particles (granules and fibers) and clumps of compact chromatin (Fig. 2a). In accordance with other species, the nucleolus was positive after staining with the regressive methods for ribonucleoproteins (Figure 2b). The presence of granules of ≈ 11 nm in diameter into the nucleoplasm, spatially related to the nucleolus was also noted (Fig. 2b, arrowheads). In addition, by using monoclonal antibodies (see materials and methods), DNA was localized mainly in the chromatin clumps surrounding the nucleolus. Only a few strands of DNA are localized within the body. (Fig. 2c). Another structure intensely labeled using this technique was the kinetoplast (data not shown), as must be expected.

**Figure 2.** Ultrastructure of *T. cruzi* intranuclear material. (a) Uranyl-lead staining , (b) Bernhard's staining for ribonucleoproteins, (c) immunolocalization for DNA. Ch, chromatin; Cy, cytoplasm; F, fibrillar component; G, granular component; Ne, nuclear envelope; N, nucleus; Nu, nucleolus; r, ribosomes. Bar: 500 nm.

Furthermore, we tested whether the ribonucleoprotein fibrogranular body we recognized as nucleolus was positive to the silver staining method for nucleolar organizer. AgNOR proteins were localized in the fibrillar component of the nucleolus (Figure 3). Distribution of AgNOR proteins showed the existence of very discrete nucleolar subcompartments (Fig. 3a, b). Additionally, nuclear bodies of ≈100 nm in diameter intensely impregnated were found. Such bodies are usually in proximity to nuclear pores or next to the nucleolus (Figs. 3a, b arrowheads). In fact, these bodies can be visualized in samples by using conventional staining methods (Fig. 3c arrowhead).

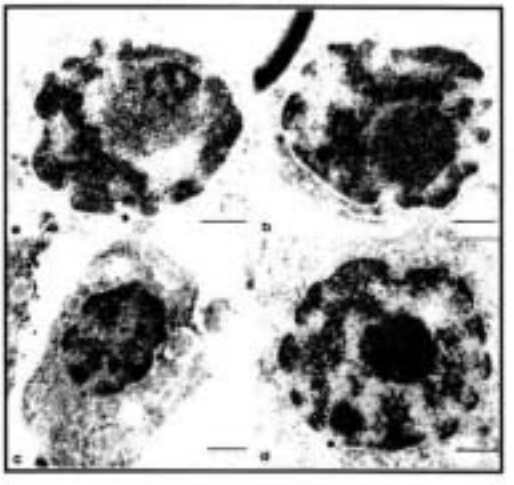

**Figure 3.** Ultrastructural silver staining of *T. cruzi*. Ag-NOR proteins are observed in the fibrogranular material within the nucleus (a-b). Uranyl-lead contrast (d). Nu, nucleolus. Bar: 250 nm.

Serial sections analysis of the whole nucleus shows clumps of compact chromatin surrounding the nucleolus. To see if there was DNA penetrating the fibrogranular material, we use computer assisted overlapped sections. 3D reconstruction showed that chromatin extends to the nucleolus presenting sites of contact with it (Fig. 4a). 3D reconstruction based on boxels allowed us to display a nuclear region containing the entire nucleolus and to perform quantitative analyses. This computing system has the capacity to make virtual "windows" through the 3D display in order to identify spatial relations among different structures (Fig. 4c). Mean volume of the nucleoli studied was 0.71 $\mu m^3$, occupying around 5.7 % of the total nuclear volume. Volume measurements from twenty nuclei studied are shown in Table 1. In order to identify the nucleolar components, every single section of the entire nucleoli studied were analyzed. No fibrillar centers were found in any of the samples serially sectioned. Granular and fibrillar components were labeled using different colors (gray and yellow respectively) and followed through the nucleolus. Both components are distributed as a continuos network through the nucleolus interacting between them and with surrounding nucleoplasm (Fig. 4b).

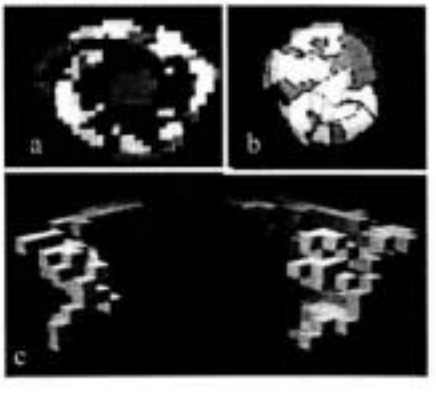


**Figure 4.** Computational display of *T. cruzi* nucleus and its components. (a) nuclear sections overlapping, (b) nucleolar sections overlapping, (c) window through the nuclear 3D reconstruction.

Table **1**. Morphology measurements of *T. cruzi* nucleoli serially cut and reconstructed

| Sample number | Nuclear volume $\mu m^3$ | Nucleolar volume $\mu m^3$ | % of nuclear volume occupied |
|---|---|---|---|
| 1 | 10.771 | 0.407 | 3.785 |
| 2 | 9.417 | 0.589 | 6.254 |
| 3 | 9.203 | 1.436 | 15.612 |
| 4 | 8.379 | 0.356 | 4.258 |
| 5 | 8.784 | 0.288 | 3.286 |
| 6 | 16.838 | 0.860 | 5.109 |
| 7 | 19.510 | 0.998 | 5.117 |
| 8 | 8.181 | 0.623 | 7.622 |
| 9 | 10.771 | 0.555 | 5.158 |
| 10 | 20.580 | 0.589 | 2.861 |
| 11 | 23.624 | 0.463 | 1.960 |
| 12 | 8.379 | 0.407 | 4.865 |
| 13 | 8.992 | 0.248 | 2.763 |
| 14 | 26.955 | 1.987 | 7.374 |
| 15 | 27.834 | 1.098 | 3.945 |
| 16 | 14.137 | 1.204 | 8.518 |
| 17 | 14.137 | 1.767 | 12.500 |
| 18 | 9.855 | 1.150 | 11.673 |
| 19 | 12.508 | 1.150 | 9.197 |
| 20 | 6.044 | 0.623 | 10.317 |
| Mean | 12.460 | 0.712 | 5.714 |
| Standard deviation | 6.606 | 0.494 | 3.691 |

**Discussion**

There are few studies that addressed the nuclear structure of trypanosomes (Esponda et al., 1983; Jiménez-García et al., 1989; Chung et al., 1990; Ogbadoyi et al., 2000) . Ribosomal biogenesis is an essential event in all living cells and the knowledge of nucleolar structures related with this process has contributed on the understanding of its regulatory steps. Although a recent study showed variation in nucleolar size, there are no data on nucleolar compartmentalization using cytochemical methods, which may complement morphological information on ribosome biogenesis.

The nucleolus of *T. cruzi* is compartmentalized. Three different criteria have been taken into account to arrive to this conclusion. 1) The electron dense material observed in the center of the nucleus of *T. cruzi* after standard transmission electron microscopy is composed of fibrogranular elements. 2) This fibrogranular material was positive after the regressive method for ribonucleoproteins. It is interesting to note that in addition of nucleolar contrast after the regressive staining, granules of ≈11 nm in diameter were also observed in the nucleoplasm. Such granules are similar in size and morphology to cytoplasmic ribosomes (Fig. 2b). Although it is

possible to recognize portions of dense fibrillar and granular components, no recognizable fibrillar centers were observed in our samples. To test if a three dimensional reconstruction would give us information whether or not fibrillar centers were localized in peripheral areas of the nucleouls, we performed serial sectioning and computer 3D reconstruction of nucleoli. In this conditions again, no firbillar centers were observed. This is not the first report on the lacking of fibrillar centers. The absence of this nucleolar subcompartment has been noticed in other cell types of different organisms (Thiry and Goessens, 1996). The analysis of the nucleolus by serial sectioning also revealed that this organelle is present as a single, spherical and small (0.7 $\mu^3$ mean volume) structure per each cell. Having one nucleolus per cell is a very common condition in higher eukaryotes though the nucleolus number might depend on the cellular cycle phase, even in the same tissue. 3) Ultrastructural localization of AgNOR proteins was shown in this same structure, mainly distributed in the fibrillar areas. This technique is an accurate cytochemical method to definitively identify nucleolar elements in the cell nucleus. In addition to the silver staining for nucleolar organizer, we observed discrete impregnation in the surrounding nucleoplasm as ≈ 100 nm in diameter nuclear bodies. 4) After high resolution immunolocalization of DNA using commercial antibodies, label was observed in the nucleoplasm in areas corresponding to chromatin, but very few gold granules were seen in the putative nucleolus, similar to other systems including plants (Martin et al., 1998). The amount of nucleolar DNA is very low in comparison to that of the entire nucleus.

Regarding the non-nucleolar intranuclear material positive after AgNOR staining and the regressive method for RNPs, it is interesting to mentions that the presence of extranucleolar particles enriched on AgNOR proteins had been reported previously (Esponda et al., 1983), but their relevance was not discussed. On the basis of the characteristics shown in this work as to the morphology and proximity to the nucleolus, their ribonucleoprotein composition, and the presence of silver staining proteins, we suggest that they may correspond to Cajal bodies. Cajal bodies are ubiquitous structures in the nucleus of eukaryotes that are involved in nuclear RNA metabolism, although the precise role has not been elucidated (Gall, 2000).

It is tempting to speculate as to the presence of a nucleolar structure as that described here early in evolution, because *T. cruzi* is considered to be a very early divergent protozoan organisms based on its phylogenetic position after using comparison of ribosomal sequence (Sogin et al., 1989).

Novel aspects of the cell biology of the nucleolus in *T. cruzi* remain to be studied as for example the nucleologenesis and the number of nucleolar organizer, in order to produce a more complete morphological counterpart to that of given by the molecular biology. Also, it would be interesting to study the causes of the reported absence of a nucleolus in the infective forms of this parasite (Elias et al., 2001).

On the other hand, vertebrates present fibrillar centers as anchoring sites for thousands of copies of ribosomal genes, separated for non transcribed spacers (NTS) of around 2.0 kb (Enright and Sollner-Webb, 1994) . *T. cruzi* ribosomal genes are present in around 100 copies (Castro et al., 1981), but separated by a NTS as long as 20 kb (Hernández et al., 1988). Therefore, fibrillar centers in vertebrates may be the result of a high number of ribosomal genes anchored in a close position, and are not present in organisms with longer spacers as *T. cruzi*.

CONCLUSIONS

We have shown here that in *T. cruzi* epimastigotes, an intranuclear and central positioned fibrogranular, ribonucleoprotein structure is present that contains few amount of DNA but is intensely impregnated with silver staining for nucleolar organizer. Therefore, this structure correspond to an authentic compartmentalized nucleolus lacking fibrillar centers. In addition nuclear bodies containing nucleolar proteins were observed that we suggest correspond to Cajal bodies.

**Acknowledgments**

The authors wish to thank Juliana Herrera for technical assistance on cell cultures and Sandra Ramos for helping us with Figure 1. G. L-V was supported by a fellow from DGEP-UNAM and PAEP-UNAM grant (101314). Partially supported by CONACyT (37620M) and DGAPA-UNAM IN221202.

**References**

Agabian N (1990) Trans-splicing of nuclear pre-mRNAs. *Cell* 61:1157-1160.

Bernhard W (1969) A new staining procedure for electron microscopical cytology, *J Ultrastruct Res*, 27:250-258.

Busch H, Smetana K (1970) *The Nucleolus*, , New York: Academic Press , pp 626.

Castro C, Hernández R, Castañeda M (1981) *Trypanosoma cruzi* ribosomal RNA: internal break in the large molecular mass species and number of genes. *Mol Biochem Parasitol* 2:219-233.

Chung HM, Shea C, Fields S, Taub RN, Van der Ploeg LH, Tse DB (1990) Architectural organization in the interphase nucleus of the protozoan *Trypanosoma brucei*: location of telomeres and mini-chromosomes, *EMBO J*, 9:2611-2619.

Djikeng A, Ferreira L, D'Angelo M, Dolezal P, Lambl T, Murta S,. Triggs V, Ulbert S, Villarino A, Renzi S, Ullu E, Tschudi C (2001) Characterization of a candidate *Trypanosoma brucei* U1 small nuclear RNA gene, *Mol Biochem Parasitol*, 113:109-115.

Dunbar DA, Wormsley S, Lowe TM, Baserga SJ (2000) Fibrillarin-associated Box C/D Small Nucleolar RNAs in *Trypanosoma brucei*. Sequence conservation and implications for2'-O-ribose methylation of rRNA, *J Biol Chem*, 275:14767-14776.

Elias MCOB, Marques-Porto R, Freymüller E, Schenkman S (2001) Transcription rate modulation through the *Trypanosoma cruzi* life cycle occurs in parallel with changes in nuclear organisation, *Mol Biochem Parasitol*, 112: 79-90.

Enright C, Sollner-Webb B (1994) Ribosomal RNA processing in vertebrates. In *RNA processing. A practical approach*, Higgins, S. J. & Hames, B. D. (Eds.), USA: Oxford University Press. pp. 135-171

Esponda P, Souto-Padrón T, De Souza W (1983) Fine structure and cytochemistry of the nucleus and the kinetoplast of epimastigotes of *Trypanosoma cruzi*. *J Protozool*. 30:105-110.

Gall JG (2000) Cajal bodies: the first 100 years, *Annu. Rev. Cell Dev. Biol*. 16:273-300.

Goodpasture C, Bloom SE (1975) Visualization of nucleolus organizer regions in mammalian chromosomes using silver stain, *Chromosoma* 53:37-50.

Hartshorne T, Agabian T (1993) RNA B is the major nucleolar trimethylguanosine-capped small nuclear RNA associated with fibrillarin and pre-rRNAs in *Trypanosoma brucei*, *Mol Cell Biol* 13: 144-154.

Hernández R, Díaz-de León F, Castañeda M (1988) Molecular cloning and partial characterization of ribosomal RNA genes from *Trypanosoma cruzi*, *Mol Biochem Parasitol* 27:275-280.

Herwaldt BL(1999) Leishmaniasis. *Lancet* 2:1191-1199.

Huang S (2002) Building an efficient factory: where is pre-rRNA synthesized in the nucleolus? *J Cell Biol* 157:739-741.

Ismaïli N, Pérez-Morga D, Walsh P, Mayeda A, Pays A, Tebabi P, Krainer AR, Pays E (1999) Characterization of a SR protein from *Trypanosoma brucei* with homology to RNA-binding *cis*-splicing proteins. *Mol Biochem Parasitol* 102:103-115.
Jess W, Hammer A, Comelissen AW (1989) Complete sequence of the gene encoding the largest subunit of RNA polymerase I of *Trypanosoma brucei*. *FEBS Lett.* 249 123-128.
Jiménez-García LF, Elizundia JM, Lopez-Zamorano B, Maciel A, Zavala G, Echeverría OM, Vázquez-Nin GH (1989) Implications for evolution of nuclear structures of animals, plants, fungi and protoctists, *Biosystems* 22:103-116
Jordan EG, Cullis CA (1982) *The nucleolus*, USA: Cambridge University Press, pp 218.
Lamond AI, Earnshaw WC (1998) Structure and function in the nucleus. *Science* 280:547-87
López-Velázquez G, Márquez J, Ubaldo E, Corkidi G, Echeverría OM, Vázquez-Nin GH (1996) Three dimensional analyses of the arrangement of compact chromatin in the nucleus of G0 rat lymphocytes, *Histochem Cell Biol* 105:153-161.
M Thiry, Goessens G (1996) *The nucleolus during the cell cycle*, Texas: Chapman & Hall Press, 101-127.
Martin M, Moreno Díaz de la Espina S, Medina FJ (1998) Immunolocalization of DNA at nucleolar structural components in onion cells, *Chromosoma* 98:368.
Misteli T (2001) Protein dynamics: implications for nuclear architecture and gene expression. *Science* 291:843-847.
Ogbadoyi E, Ersfeld K, Robinson D, Sherwin T, Gull K (2000) Architecture of the *Trypanosoma brucei* nucleus during interphase and mitosis, *Chromosoma* 108:501-513.
Risueño MC, Medina FJ (1986) *The nucleolar structure in plat cells*, Universidad del Pais Vasco, pp 154.
Roth J (1986) Post-embedding cytochemistry with gold-labeled reagents. A review. *J. Microsc.* 143:125-137.
Scheer U, Hock R, (1999) Structure and function of the nucleolus, *Curr Opin Cell Biol* 11: 385-390.
Schwarzacher HG, Mosgoller W, (2000) Ribosome biogenesis in man: current views on nucleolar structures and function, *Cytogen Cell Genet* 91:243-254.
Shaw P, Jordan GE (1995) The nucleolus. *Annu Rev Cell Dev Biol* 11: 93-121.
Sogin M, Gunderson JH, Elwood HJ, Alonso R, Peattie DA (1989) Phylogenetic Meaning of the Kingdom Concept: An Unusual Ribosomal RNA from *Giardia lamblia Science* 243: 75-77.
Spector DL (1993) Macromolecular domains within the cell nucleus. *Annu Rev Cell Biol* 9:265-315
Spector DL (2001) Nuclear domains. *J Cell Sci* 114: 2891-2893.
Spector DL, Goldman RD, Leinwand LA (1998) *Cells: a laboratory manual*, New York,Cold Spring Harbor laboratory Press, pp 2136.
Thiry M, Goessens G (1996) Nucleolar Functional Organization. In *The nucleolus during the cell cycle*, Chapman & Hall Press Texas, pp 101.127.
Vázquez-Nin GH, Echeverría OM (2000) *Introducción a la microscopía electrónica aplicada a las ciencias biológicas*. Universidad Nacional Autónoma de México-Fondo de Cultura Económica, pp.168.
Wagner W, So M (1990) Genomic variation of *Trypanosoma cruzi*: involvement of multicopy genes, *Infect Immun* 58: 3217-3224.
Wettstein R, Graver A (1973) Film-supporting frames for mounting section grids, *J. Ultrastruct Res* 43:436-447.
World Health Organization, Progress 1995-1996, (1997) *Thirteenth program report of the UNDP/World Bank/WHO Special Program for Research and Training in Tropical Diseases*, pp 112-123.